MAY 1 6 1983

Mr. Chris H. Poindexter
Vice President, Engineering and
Construction
Baltimore Gas and Electric Company
P. O. Box 1475
Baltimore, Maryland 21203

Dear Mr. Poindexter:

This letter is in response to your proposal regarding Baltimore Gas and Electric's (BG&E) participation in the activities related to Unresolved Safety Issue A-47, "Safety Implications of Control Systems." A key part of the Task Action Plan for this issue is the analysis of postulated plant transients assuming various control system failures. The specific computer analyses to be performed would be determined from failure modes and effects analyses of the control systems. The performance of these analyses requires a considerable amount of design detail that is not contained in plant FSARs. You have stated that significant manpower and resources, that are needed for other priority issues, would be expended in obtaining and providing this information to the staff, and in the necessary followup to assure that it is correctly applied in modeling Calvert Cliffs on a hybrid simulator, to be utilized by our contractor (ORNL). At a meeting between NRC staff and your representatives held on April 13, 1983, and in your letter to me dated April 14, 1983, BG&E proposed an alternate approach in which the computer analyses would be performed on the Calvert Cliffs plant-specific simulator currently under development by Combustion Engineering.

We believe that your proposal has merit, and accept the suggestion in your letter to discuss this matter further with BG&E and Combustion Engineering. Discussion of the following matters would improve our understanding of your proposal.

(1) Discussion of the methods and models incorporated by Combustion Engineering in the plant simulator. We wish to compare the capabilities of the models of the Calvert Cliffs plant simulator with those models being developed by our contractor (ORNL), and more particularly, to assess the capability of the Calvert Cliffs simulator to perform the necessary analysis of the potential consequences of control system malfunctions.

(2) Discussion of potential NRC staff involvement, on an audit basis, during the check-out phase of the final verification testing of the Calvert Cliffs simulator.

(3) Discussion of how the staff and their contractor would participate in, and witness, the actual running of the transient studies at the simulator location. We would expect that the NRC would specify the failure scenarios of the control systems under various plant operating conditions and/or events that will be studied on the simulator. In

XA

OFFICE ▶				XA Copy Has Been Sent to PDR		
SURNAME ▶	8305250555					
DATE ▶						

order to accomplish this task, access to plant-specific system design information would be needed by the staff.

(4) Discussion of the extent of Combustion Engineering's participation and assistance in providing technical support to this program.

(5) Discussion of the schedules for: (a) the completion of the simulator, (b) the verification testing, and (c) the expected availability for the staff and their contractors to perform the studies.

Your proposal for a meeting during the week beginning May 23 is acceptable. However, we request that this initial meeting be held in Bethesda to enable fuller participation by NRC management, the USI A-47 reviewers, and several of our contractor staff who are actively involved in the model development activities. The contractor representatives would be prepared to present a brief description of the methodology employed in the development of their models, and will assist the staff in assessing the Combustion Engineering simulator capability. In addition, the CE representatives should be prepared to describe the methodology employed in the development of their models and their simulator capability. We suggest that the meeting be held on Wednesday, May 25, 1983 at 9:00 a.m. This mid-week date would facilitate CE's and our contractor's travel schedules. Mr. Andrew Szukiewicz (302-492-4713), USI A-47 Task Manager, will contact your Mr. Rich Olson to arrange the details of the meeting.

We appreciate your willingness to pursue a timely resolution on this important program in a manner that would be mutually beneficial to both our organizations.

Sincerely,

(Signed) William J. Dircks

William J. Dircks
Executive Director for Operations

DISTRIBUTION
Central Files
GIB Rdg
DST c/f
WDircks
JRoe
TRehm
VStello
RMinogue
ECase
HDenton
PPAS
DEisenhut
RMattson
RVollmer
HThompson
NGrace
BSnyder
TSpeis
FSchroeder
KGoller
BSheron
FRosa
KKniel
PNorian
✓ ASzukiewicz
JMullin (13051)
MGarver (13051)
CTwigg (13051)
CBarnes
SDiab
ERossi
DBasdekas
DJaffee

Note: Karl Goller (RES) reviewed and concurred in draft. - FSchroeder 5/3/83

OFFICE	DST:GIB	DST:GIB	DST:GIB	DST:ADGP	DST:D	NRR	EDO
SURNAME	ASzukiewicz:db	PNorian	KKniel	FSchroeder	TSpeis	~~HDenton~~ ECase	WJDircks
DATE	5/3/83	5/3/83	5/3/83	5/3/83	5/3/83	5/ /83	5/ /83

LIST OF ATTENDEES
JUNE 1, 1983

A-47 MEETING W/BG&E

NAME	ORGANIZATION	PHONE NUMBER
A. J. Szukiewicz	NRC/NRR/DST	492-4713
T. R. Charlton	EG&G Idaho	583-9324 (FTS)
S. J. Willats	BG&E	301-234-5344
S. E. Jones	BG&E	301-269-4798
R. F. Ash	BG&E	301-234-5381
J. R. Hill	BG&E	301-269-4955
M. D. Patterson	BG&E	301-234-8529
R. C. L. Olson	BG&E	301-234-6229
R. J. Spitznas	BG&E	301-234-5454
D. L. Basdekas	NRC/RES/DFO	443-5966
K. R. Goller	NRC/RES/DFO	443-5991
L. B. Marsh	NRC/NRR	492-7626
J. Guttmann	NRC/NRR/RSB	492-9442
K. Kniel	NRC/NRR/DST/GIB	492-7359
Wolfgang Wulff	BNL	516-288-2608
A. L. Lotts	ORNL	615-574-0422
O. L. Smith	ORNL	615-574-5543
N. E. Clapp, Jr.	ORNL	615-574-0417
J. P. Renier	ORNL	615-574-5258
M. Chiramal	NRC/AEOD	492-4441
E. Rossi	NRC/ICSB	492-7140
F. Rosa	NRC/ICSB	492-7141
E. Chelliah	NRC/DST/RRAB	492-8338
D. Earles	CE	203-688-1911 x9044
J. McNally	CE	203-225-2771 x 13
W. J. Gill	CE	203-688-1911 x3135
R. R. Mills	CE	203-688-1991 x4738
N. Zuber	NRC/RES	
R. Arbue	BNL	

Agenda to June 1 Meeting with BG&E

Introduction	NRC/GIB
(1) Overview of the USI A-47 objectives and task activities.	
(2) Schedule for the Calvert Cliffs Review.	
BG&E's and CE's Proposed participation in the A-47 program.	BG&E
Discussion of the Calvert Cliffs Simulator	GE
(a) Methods and models used - a description of the Neutronic and thermal hydraulic codes used.	
(b) Verification of Simulator	
(1) Type of testing	
(2) Schedule	
Discussion of the NRC use of the plant simulator to run transients	BG&E/CE
(1) Schedules	
(2) Location	
General Discussion	

ATTACHMENT 5

Handouts

A-47 Meeting with BG&E

June 1, 1983

UNRESOLVED SAFETY ISSUE TASK A-47

"SAFETY IMPLICATIONS OF CONTROL SYSTEMS"

° TASK APPROVED BY THE COMMISSION IN DECEMBER 1980

° TASK ACTION PLAN APPROVED BY NRC IN SEPTEMBER 1982

TASK OBJECTIVES

PERFORM AN INDEPTH EVALUATION OF THE NON-SAFETY GRADE CONTROL SYSTEMS THAT ARE TYPICALLY USED DURING PLANT OPERATION.

- VERIFY THE ADEQUACY OF CURRENT LICENSING DESIGN REQUIREMENTS
- PROPOSE (IF NECESSARY) ADDITIONAL GUIDELINES AND CRITERIA TO ASSURE THAT NUCLEAR POWER PLANTS DO NOT POSE UNACCEPTABLE RISK DUE TO NON-SAFETY GRADE SYSTEM FAILURES

REVIEW 4 PLANT DESIGNS OF THE MANUAL
AND AUTOMATIC NON-SAFETY GRADE
CONTROL SYSTEMS, ONE FOR EACH
OF THE NSS SUPPLIERS

B&W - OCONEE (REVIEW BY ORNL THRU RES FUNDING)

CE - CALVERT CLIFFS (REVIEW BY ORNL THRU RES FUNDING)

GE - BROWNS FERRY (REVIEW BY INEL THRU NRR FUNDING)

W - ROBINSON (REVIEW BY INEL THRU NRR FUNDING)

BOP DESIGNS OF CONTROL SYSTEMS THAT INTERFACE WITH THE NSSS DESIGN OR DYNAMICALLY INTERACT WITH THE PRIMARY REACTOR FLUID SYSTEMS AND/OR THE SECONDARY STEAM SYSTEM WILL ALSO BE REVIEWED.

METHOD

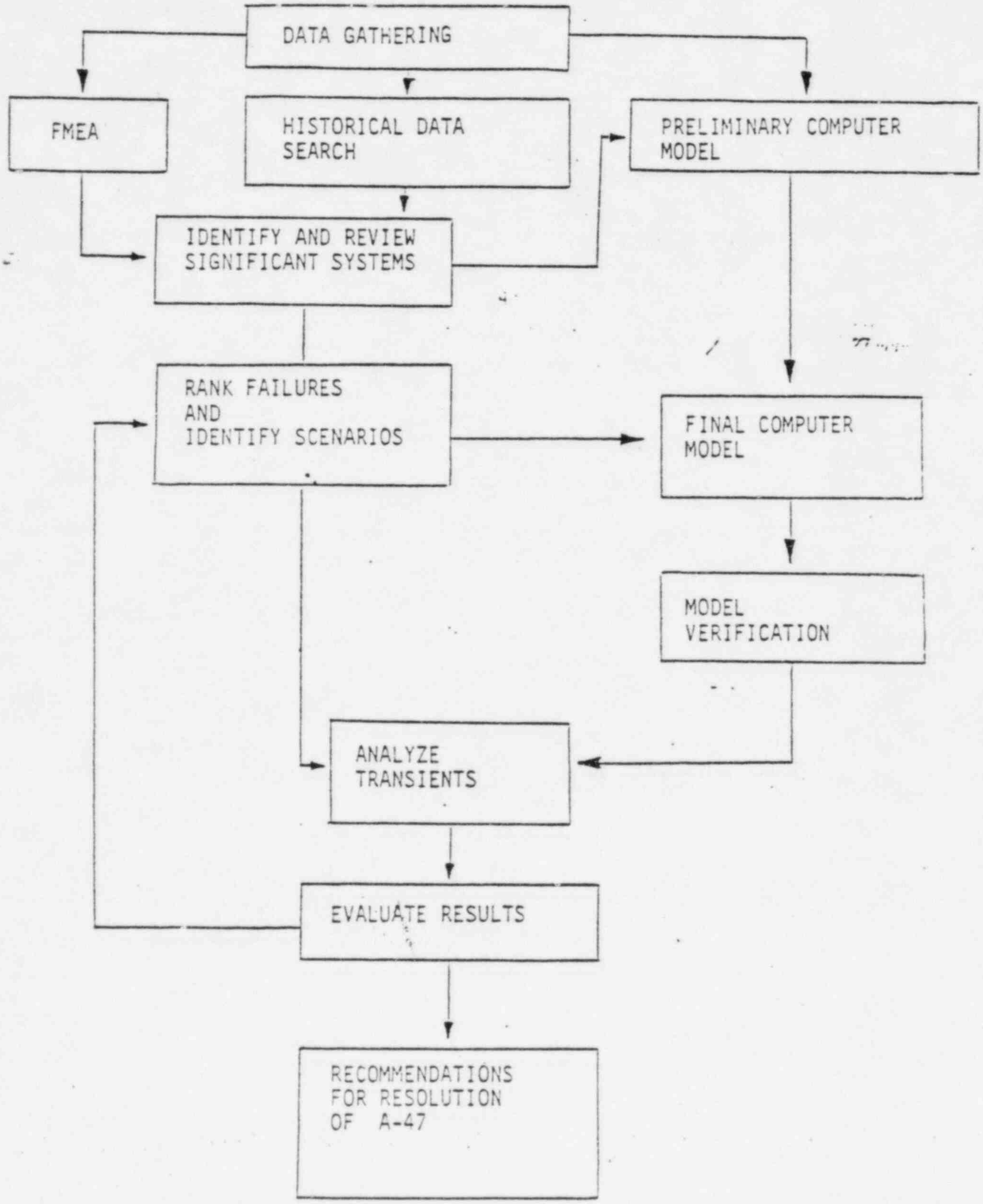
DATA GATHERING
FMEA
HISTORICAL DATA SEARCH
PRELIMINARY COMPUTER MODEL
IDENTIFY AND REVIEW SIGNIFICANT SYSTEMS
RANK FAILURES AND IDENTIFY SCENARIOS
FINAL COMPUTER MODEL
MODEL VERIFICATION
ANALYZE TRANSIENTS
EVALUATE RESULTS
RECOMMENDATIONS FOR RESOLUTION OF A-47

INITIAL SPECIAL EMPHASIS

° REACTOR VESSEL/STEAM GENERATOR OVERFILL

° REACTOR VESSEL OVERCOOLING

A-47 SCHEDULE

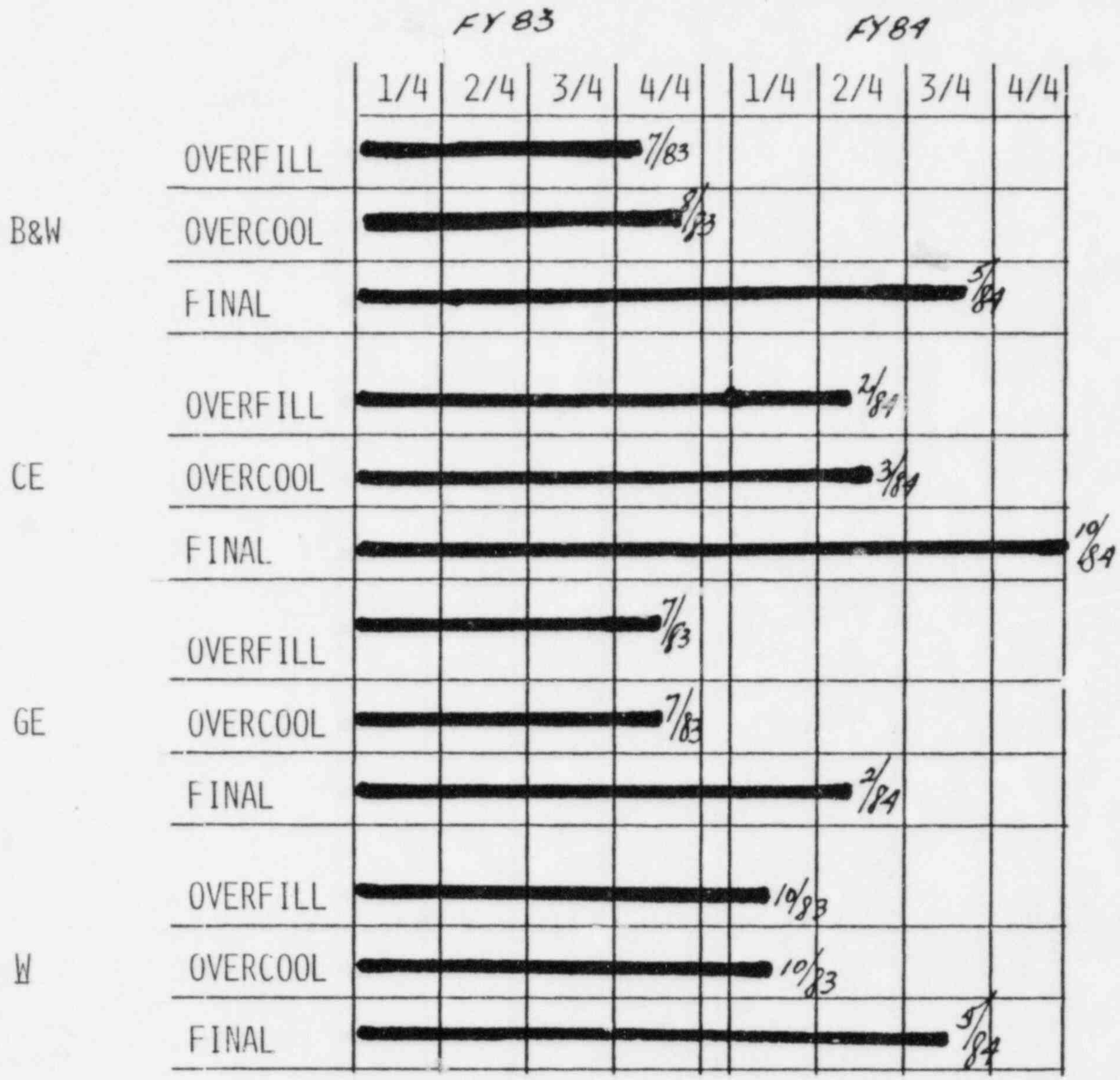

Enclosure

SUMMARY DESCRIPTION

CALVERT CLIFFS

SIMULATOR

The industry standard governing training for licensed plant operators is ANSI/ANS 3.1-1978 (formerly N18.1-1971). The Plant Simulator is designed to meet the requirements for a "suitable reactor simulator" (ANSI/ANS-3.1-1978, Section 5.2.1) and for a "simulator similar in design" (Appendix A). ANSI/ANS-3.5-1979 establishes the minimum requirements for nuclear power plant simulators. The plant simulator proposed exceeds the requirements of this standard.

CONTROL ROOM PANELS

The control panel physical arrangement, size and components will closely parallel the reference plant. Plant information will be displayed to the operator in the same form that is available in the reference plant; i.e., meters, recorders, etc. Controls, meters, alarms, recorders, switches, annunciators, controllers and other components that would function during normal and abnormal operations will be furnished in the simulator.

INSTRUCTOR'S STATION

The instructor's station will be designed to minimize the simulator system knowledge required to run the simulator. Instructors can thus concentrate their efforts on training students rather than on running a computer facility.

Multi-Processor System

The multi-processor system consists of Perkin-Elmer 32-bit processors. The four processors execute the general tasks of primary systems modeling, secondary systems modeling, I/O processing, and display processing. The Model 3244, the latest in the Perkin-Elmer series of 32-bit processors, is specifically designed for high-performance applications. The Model 3244 attains high performance through its basic architectural characteristics:

- Full 32-bit parallel architecture
- Four-way interleaved memory
- Cache Memory
- Instruction lookahead stacks
- Direct addressing to megabytes
- Writable control store (WCS)
- Memory address translator (MAT)
- Dual bus structure with fast direct memory access
- Double precision floating point hardware
- Four-level interrupt system
- Multiple register stacks
- Powerful instruction set

The customized executive system to control and coordinate program development and maintenance is known as the UNISYSTEM™. UNISYSTEM™ was developed by Power Technologies, Inc. (PTI). UNISYSTEM is made up of UNITRAN, UNIDATA, UNITEX and UNIFLOW.

POWER

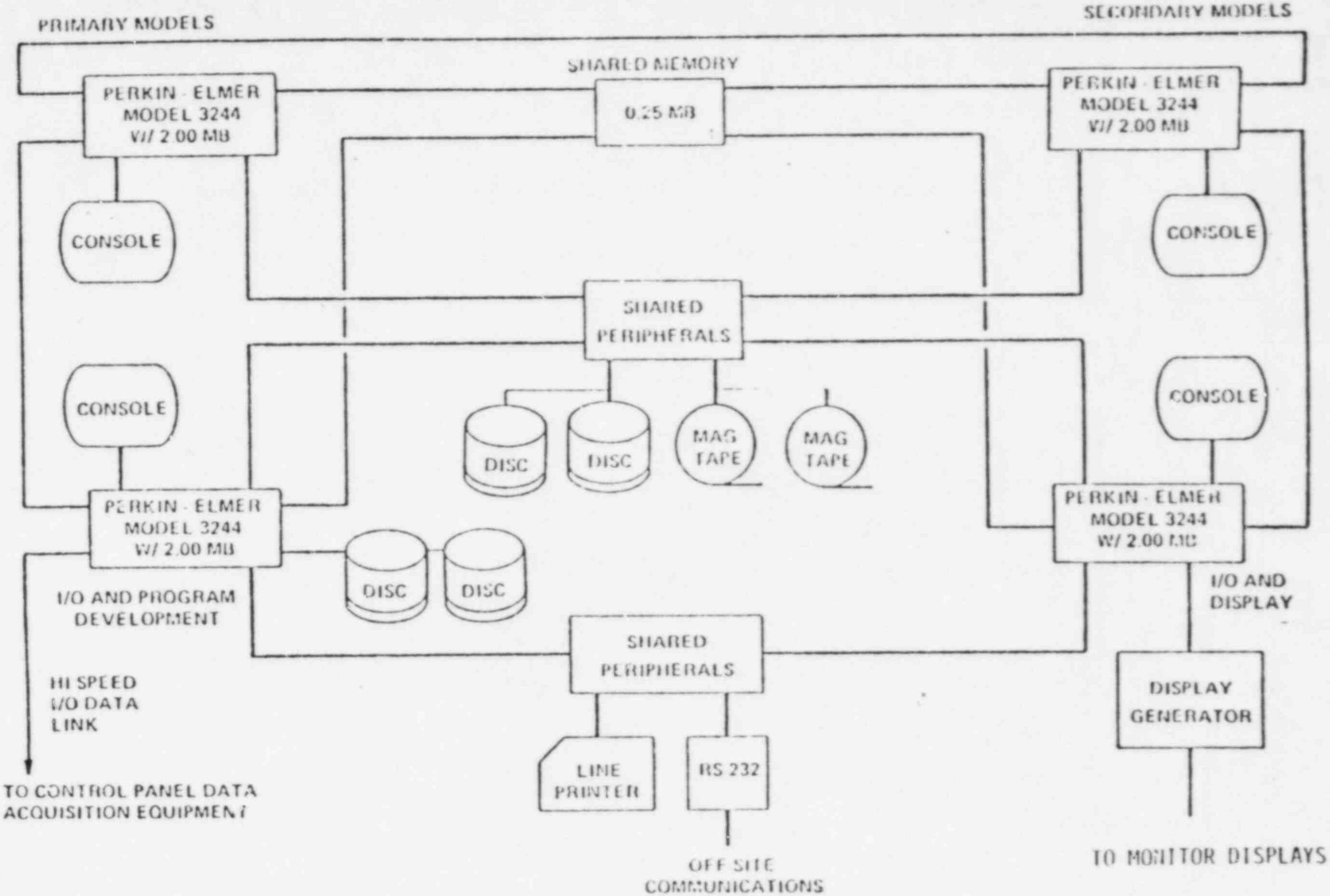

Figure

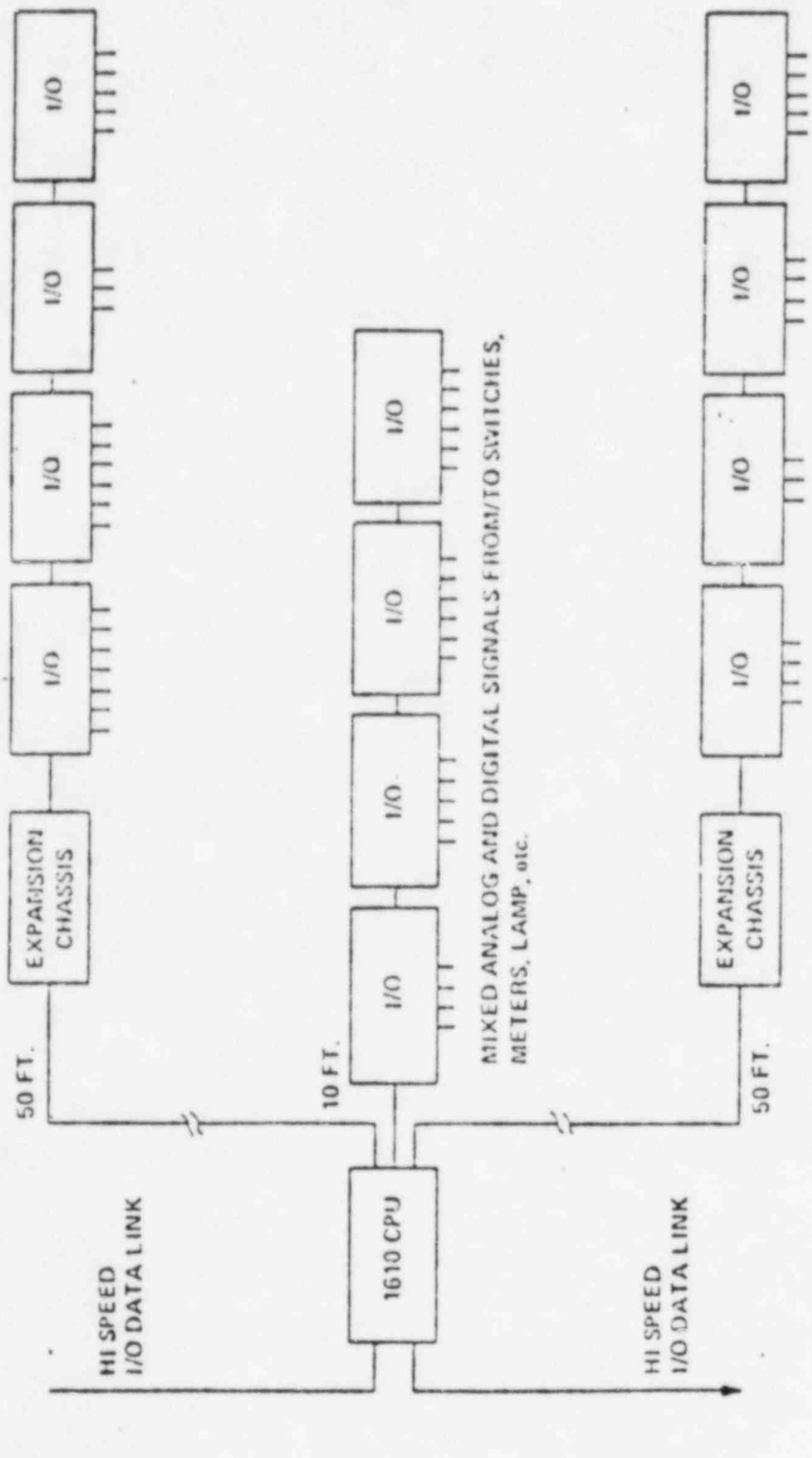

POWER SYSTEMS
COMBUSTION ENGINEERING, INC.

TYPICAL I/O DATA ACQUISITION BLOCK DIAGRAM (ONE OF FOUR)

Figure III-2

The simulator will be designed to accurately represent a broad range of combinations of conditions, procedures, malfunctions, and overrides. This is achieved while simultaneously providing the user the needed confidence that the results of any simulated occurrence are accurate.

The two criteria stated above are based on the presumption that whatever can be done from the control room may well be done at some time. If the simulator were to respond incorrectly to any of these input conditions <u>without alerting the user</u>, the net result could very well be counterproductive training of operators or incorrect conclusions drawn by other users.

The most important elements in meeting those criteria are:

1) the use of physical models based on first principles, and,

2) the incorporation of flags which alert the user any time any of the models are being used in such a way that the simulator outputs could be questionable. An example is the case that an iterative solution is used to predict a specific parameter and the convergence criterion is not met. In this case, the simulator solution will continue after appropriately alerting the user.

In summary, the C-E Simulator model and malfunction design is intended to avoid the shortcomings of past simulator modeling and malfunctions. This will be accomplished through a balanced approach of more accurate and more generalized models, combined with clear identification of any limits to simulation results. Through this approach, C-E believes that careful design rather than major technological advancement can provide a firmer foundation for the next generation of plant simulators.

Specific design models to be used in the development and/or verification of the simulator models include (but are not limited to):

- <u>CESEC</u>

  CESEC is an NSSS simulation that has been (and is continuing to be) verified with respect to actual plant measurements. Some of the dynamic functions included in this simulation are the reactor core, reactor coolant mass transport and pressurization, reactor coolant system safety valve behavior, steam generators and steam generator water level, main steam bypass, and secondary safety and turbine valve behavior.

- <u>COAST</u>

  The COAST program calculates reactor coolant flow for any combination of running, idle, and coasting reactor coolant pumps, including forward or reverse flow in any coolant leg. The conservation of momentum equation is used in each flow path for transient one-dimensional flow of an incompressible fluid. Conservation of mass equations are written for appropriate nodal points, and pressure losses due to friction, elbows and shock losses are assumed proportional to the flow velocity squared.

- <u>FLAIR</u>

  FLAIR provides a calculation of the three-dimensional power distribution in a nuclear reactor. Changes in core power distribution due to control rod position and xenon transients are accurately calculated; the effects of RCS boron concentration, pressure and temperature are included.

The organization of the plant process models is shown in Figure V-1. Each process model is associated with a control systems model as shown in Figure V-2. The interrelationship between fluid system, electrical and logic models is shown in Figure V-3. The autonomy of the process and electrical models simplify changing models to follow inevitable plant modifications.

FIGURE V-1
PROCESS MODEL STRUCTURE
AND PRINCIPAL INTERFACES

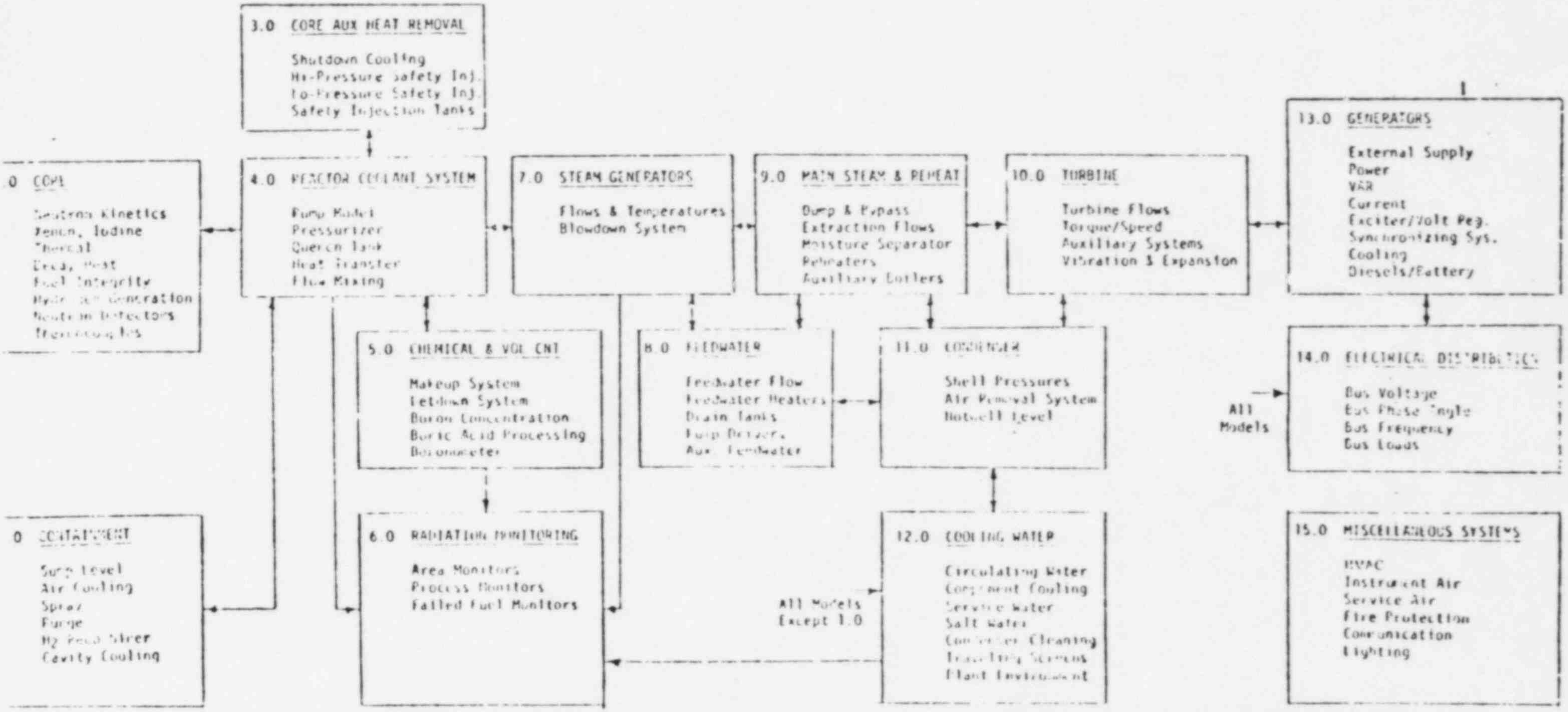

FIGURE V-2
CONTROLS MODEL STRUCTURE
AND PRINCIPAL INTERFACES

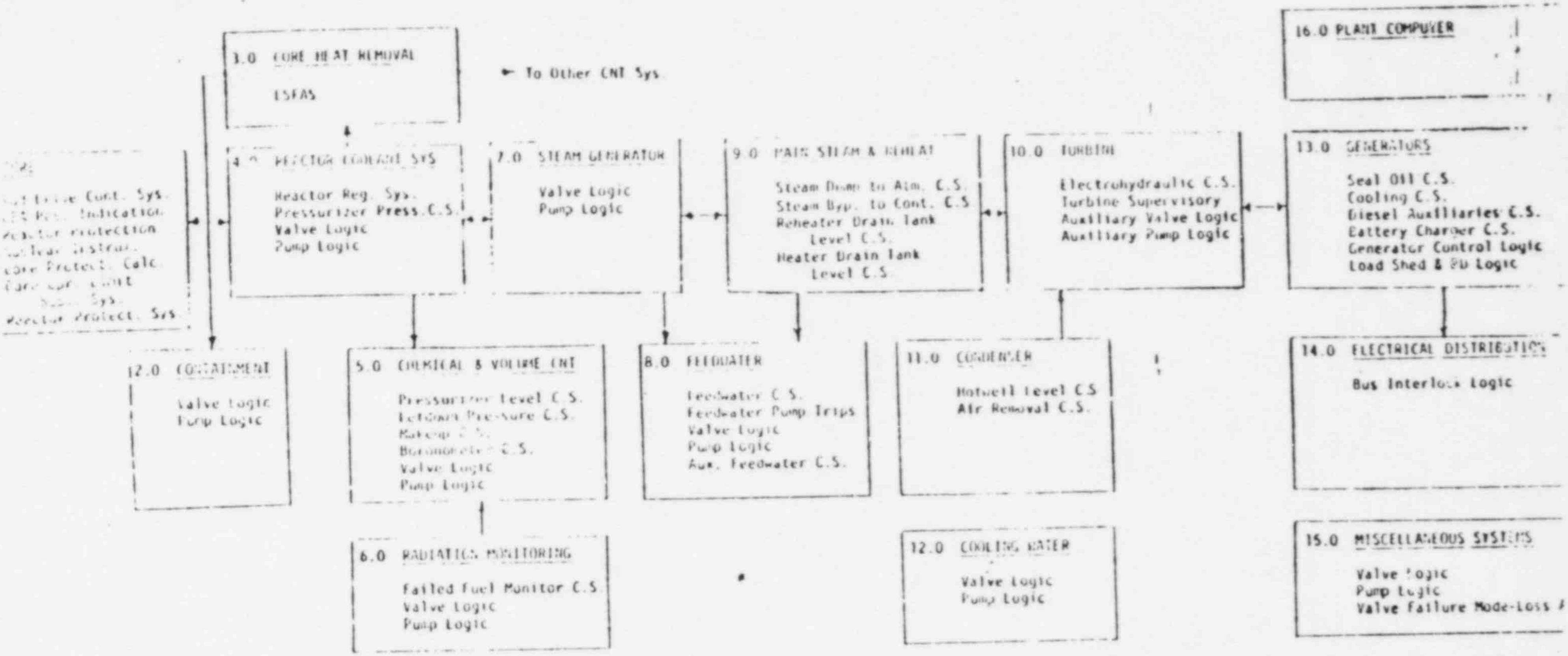

BG&E FULL SCALE SIMULATOR

I. DESCRIPTION

A. DESIGN OBJECTIVES
B. SOFTWARE/MODELS
C. HARDWARE

II. PERFORMANCE CHARACTERISTICS

A. MALFUNCTIONS
B. OVERRIDES/REMODES
C. MANUFACTURING STATUS

SPEAKERS:

PART I: WILLIAM J. GILL
MANAGER, INSTRUMENTATION SYSTEMS
COMBUSTION ENGINEERING, INC.

PART II: J. K. MCNALLY
PROGRAM MANAGER; BG&E SIMULATOR
COMBUSTION ENGINEERING, INC.

BACKGROUND

C-E WAS AWARDED A CONTRACT FOR A FULL SCALE ADVANCED SIMULATOR FOR THE BG&E CALVERT CLIFFS PLANT IN FEBRUARY OF 1981.

ADVANCED CORE, REACTOR COOLANT SYSTEM PRESSURIZER AND STEAM GENERATOR MODELS HAVE BEEN DEVELOPED IN SUPPORT OF THIS CONTRACT.

THE SIMULATOR IS IN THE LATER STAGES OF INTEGRATION AT THE C-E FACILITIES IN NEW BRITAIN CONNECTICUT. ACCEPTANCE TESTING IS SCHEDULED FOR LATE THIS YEAR.

C-E ADVANCED SIMULATOR CONCEPT

1. OPERATOR PERFORMANCE IS SIGNIFICANTLY ENHANCED BY TRAINING IN "PROBLEM SOLVING" TECHNIQUES.

2. THIS REQUIRES THE SIMULATION OF A LARGE SPECTRUM OF ACCIDENTS AND MULTIPLE FAILURES WHICH THE OPERATOR HAS NOT PREVIOUSLY SEEN.

3. SIMULATOR MODELS DEVELOPED FROM THE C-E DESIGN CODES ARE USED TO AVOID "MODEL BREAKDOWN" DURING THESE TYPES OF EVENTS.

4. THE C-E SIMULATOR IS BASED ON THESE PRINCIPLES.

SIMULATOR MODEL DEVELOPMENT

C-E APPROACH	TYPICAL APPROACH
C-E DESIGN MODELS	
↓	
SIMPLIFY FOR REAL TIME	
↓	
FINAL SIMULATOR MODEL	
	FINAL SIMULATOR MODEL
	↑
	INCREASE COMPLEXITY TO OBTAIN FIDELITY
	↑
	SIMPLIFIED MATH MODELS DUE TO COMPUTER LIMITS
	↑

THE USE OF DESIGN MODELS RESULTS IN A WIDER SPECTRUM OF EVENTS WHICH CAN BE MORE REALISTICALLY SIMULATED.

SIMULATION SOFTWARE

THE SIMULATOR SOFTWARE IS COMPRISED OF:

1. PERKIN-ELMER OPERATING SYSTEM

2. UNISYSTEM

3. ALGORITHM BASED ON THE DESIGN CODES

APPROXIMATELY 98% OF THE SOFTWARE IS IN FORTRAN

C-E MODEL EXPERIENCE

C-E HAS DEVELOPED POWER PLANT SIMULATION MODELS TO SUPPORT THE SAFETY AND PERFORMANCE ANALYSES.

IN EXCESS OF 100 MAN-YEARS OF DEVELOPMENT HAVE BEEN INVESTED TO OBTAIN ACCURATE FAST RUNNING CALCULATIONS.

THESE MODELS HAVE BEEN AND WILL CONTINUE TO BE COMPARED WITH FIELD AND INDUSTRY TEST DATA. IMPROVEMENTS HAVE BEEN MADE WHERE NECESSARY.

REACTOR CORE MODEL

DESIGN BASIS: PROVIDE ACCURATE REAL-TIME 3-D CORE POWER DISTRIBUTION CALCULATION WITHOUT USING EXCESSIVE COMPUTER TIME.

IMPLEMENTATION:

1. BASED ON C-E DESIGN CODE "FLAIR", MODIFIED FOR SIMULATOR USE.

2. ONE-GROUP MULTI-NODE DIFFUSION MODEL.

3. INNOVATIVE IMPROVED QUASISTATIC METHOD (IQSM) WITH 132 (4 AXIAL, 33 RADIAL) NODES.

4. USES LESS THAN 250 MS./SEC.

CEFLASH

- CEFLASH IS USED AS THE BASIS FOR THE SIMULATOR RCS LOOP AND VESSEL MODEL
- ORIGINALLY DESIGNED FOR USE IN SMALL LOCA ANALYSIS
- USES THERMAL-HYDRAULIC NODE-FLOW PATH NETWORK FOR SOLVING MASS, ENERGY, AND MOMENTUM EQUATIONS
- SOLVES 2-PHASE NON-EQUILIBRIUM CONDITIONS (TMI)
  - VOID FORMATION, TRANSPORT AND COLLAPSE
  - COUNTER-FLOW OF STEAM AND LIQUID
  - REVERSE FLOW
  - UNCOVERED CORE

RCS SIMULATOR NODE DIAGRAM

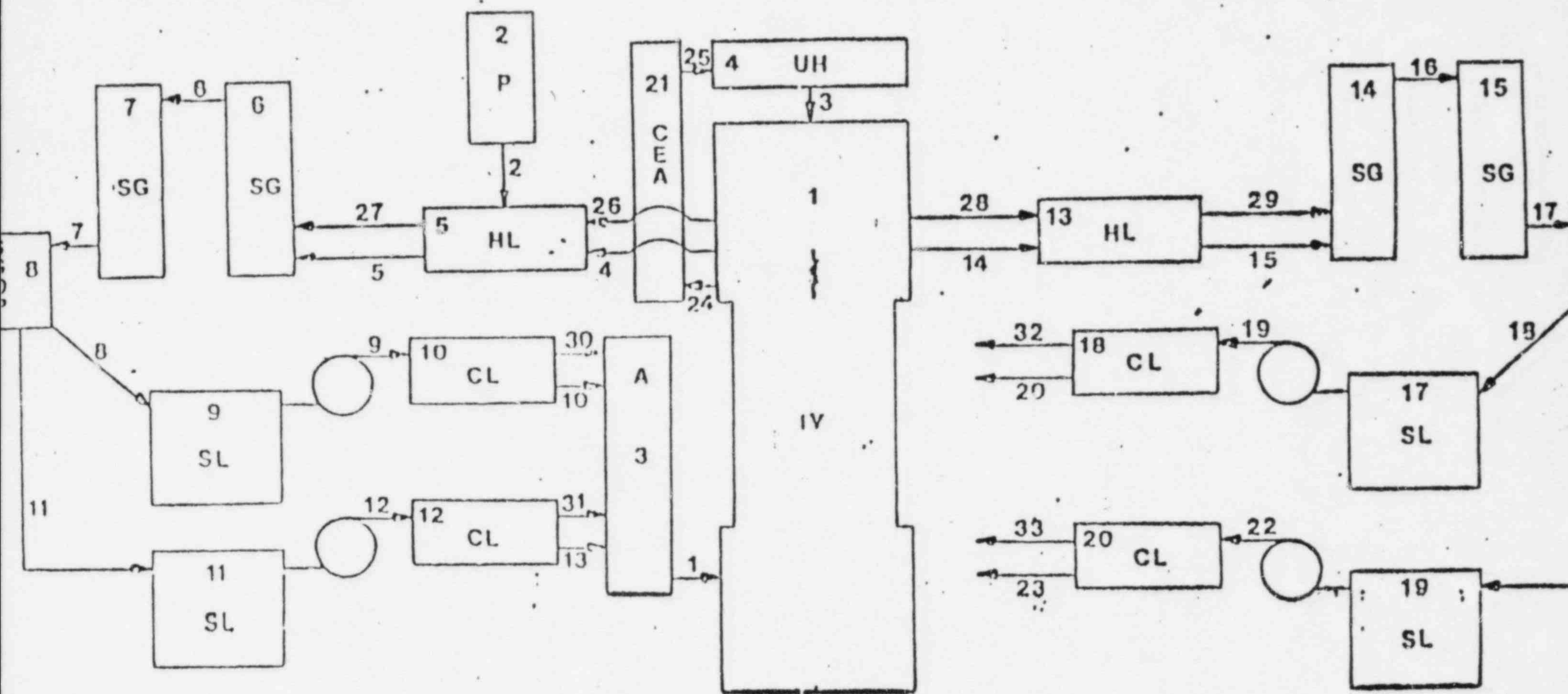

STEAM GENERATOR MODEL

- o DEVELOPED FROM DESIGN MODEL USED IN "LTC" NSSS CODE
- o "LTC" CODE USED FOR DESIGN ANALYSIS OF LONG TERM STEAM LINE BREAK TRANSIENTS, SYSTEM LOAD CHANGES, AND OTHER SYSTEM PERTURBATIONS
- o TEST RESULTS COMPARE FAVORABLY WITH PLANT DATA (ANC-2)
- o ACCURATE SHRINK AND SWELL CALCULATIONS
- o REALISTIC LEVEL SIMULATION ADVANTAGE FOR OPERATOR TRAINING IN CONTROLLING LEVEL

CODE DEVELOPMENT APPROACH

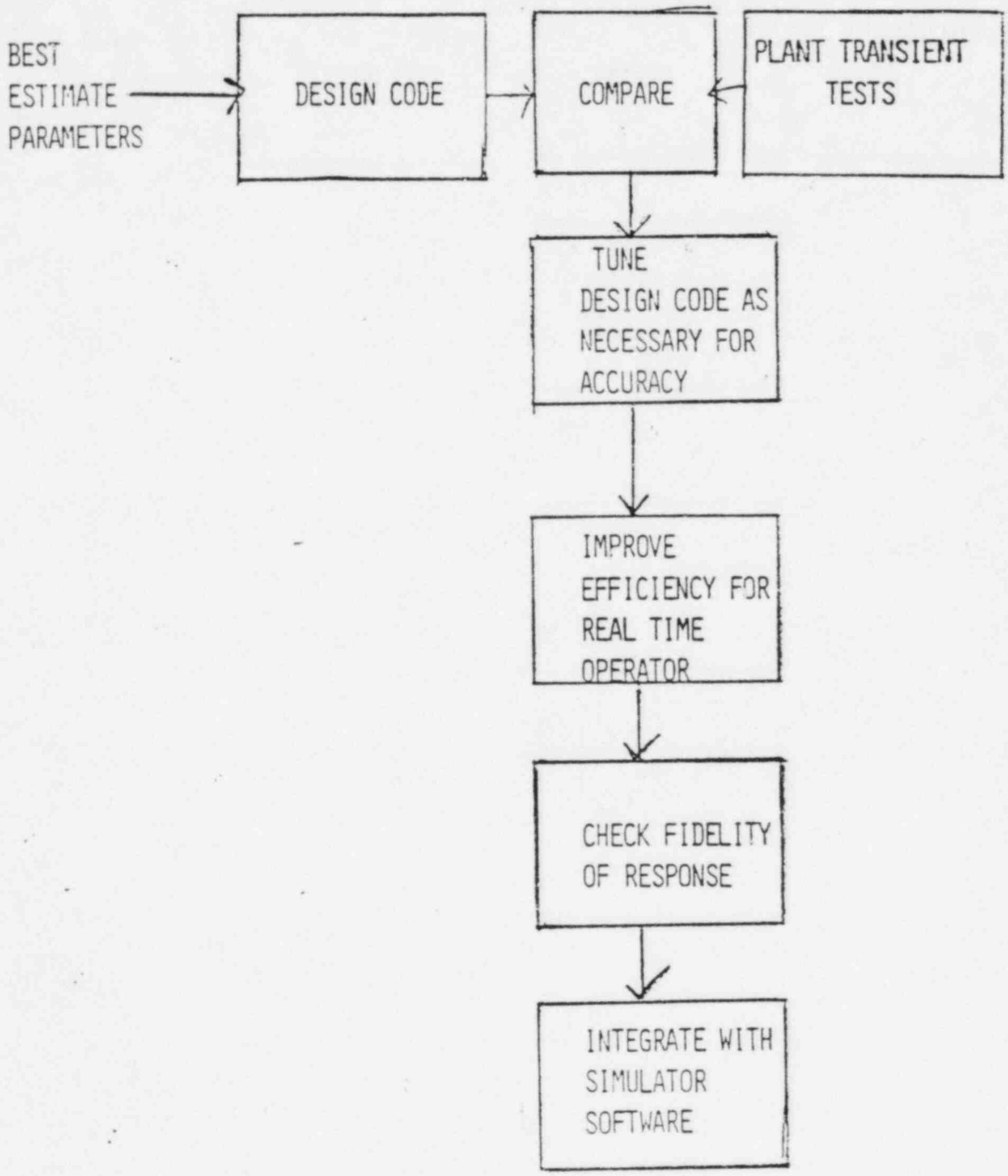

SIMULATOR RCS MODEL

FLASH METHODOLOGY APPROACH

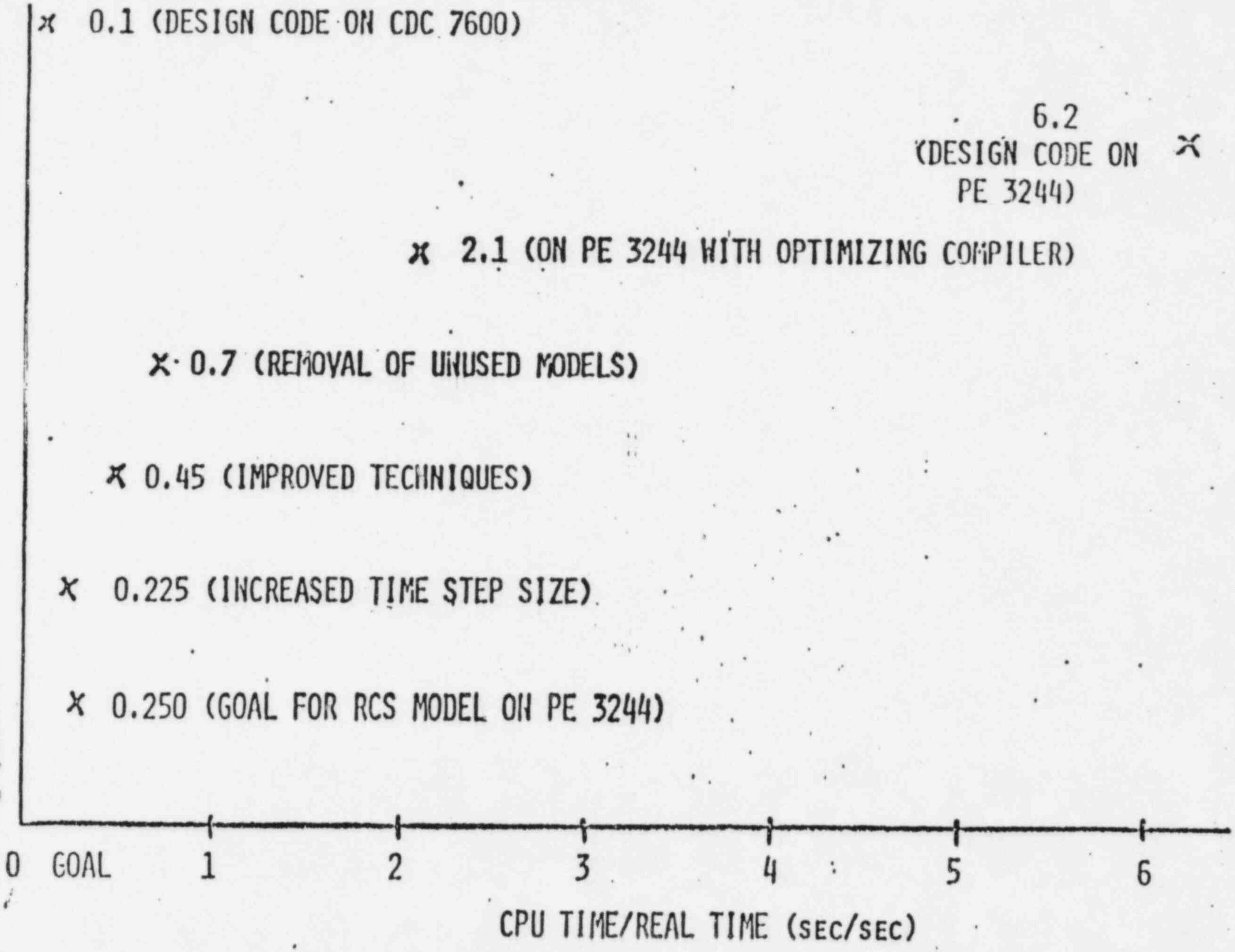

VERIFICATION OF MODEL VALIDITY
(3-STEP APPROACH)

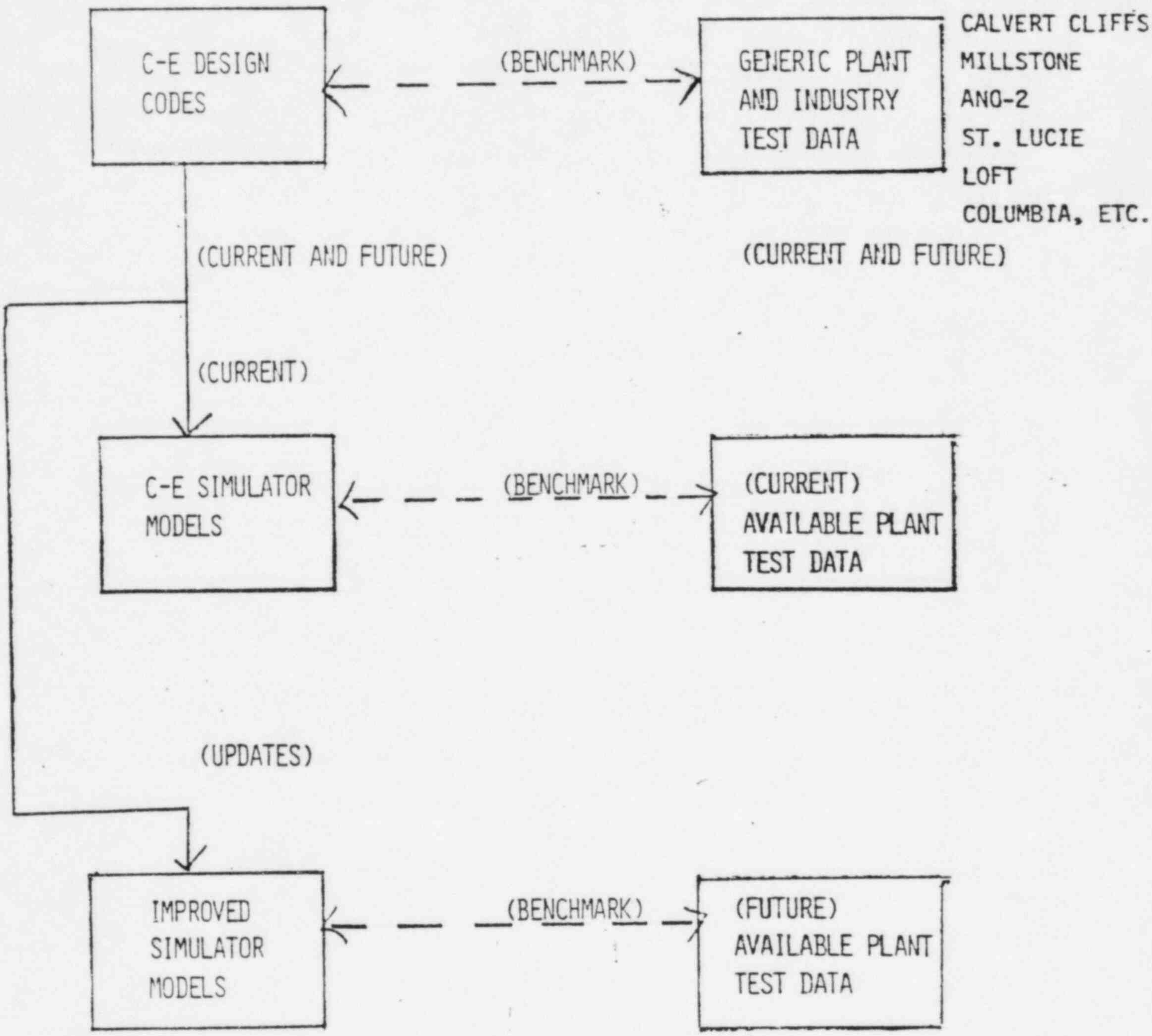

TURBINE TRIP FROM 100% POWER (LONG TERM RESPONSE)

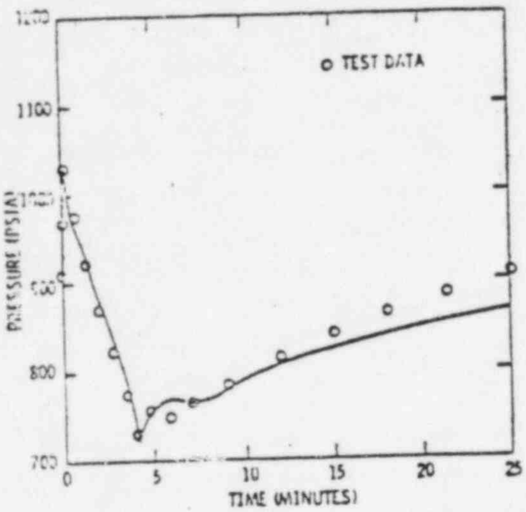

Fig. 7. Steam Generator A Pressure

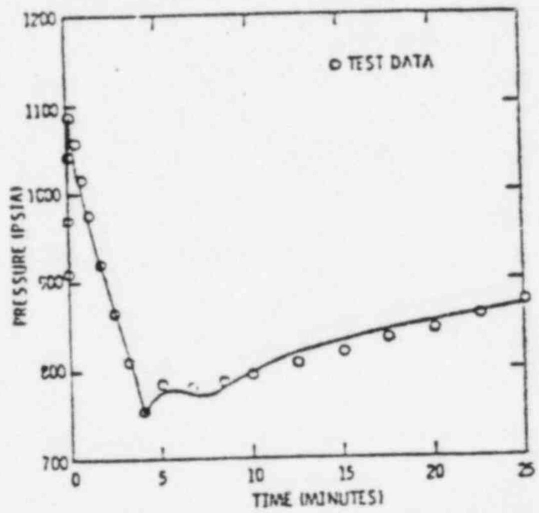

Fig. 8. Steam Generator B Pressure

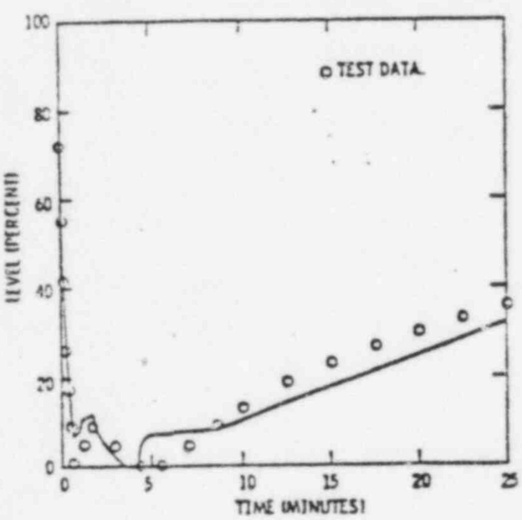

Fig. 9. Steam Generator Level

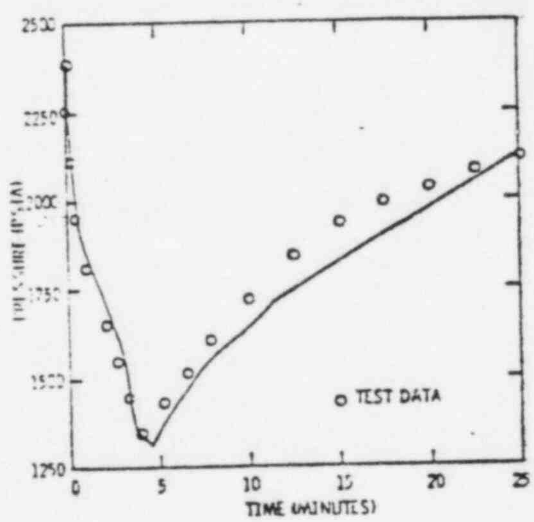

Fig. 10. Pressurizer Pressure

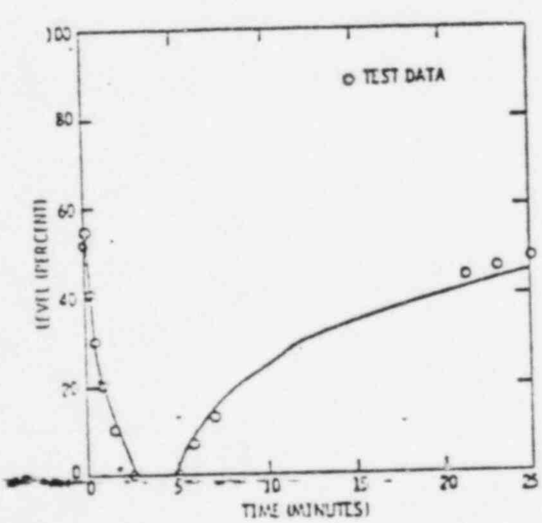

Fig. 11. Pressurizer Level

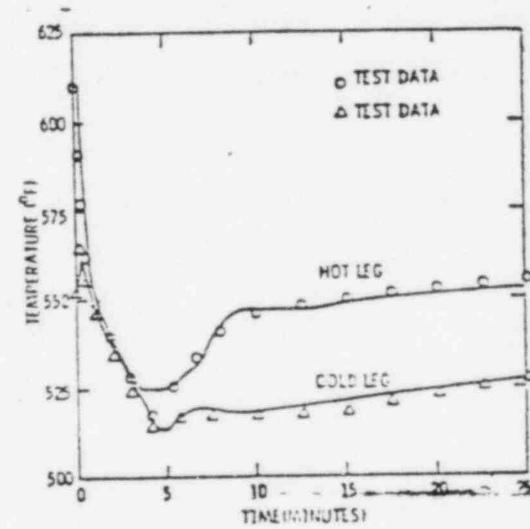

Fig. 12. RCS Temperatures

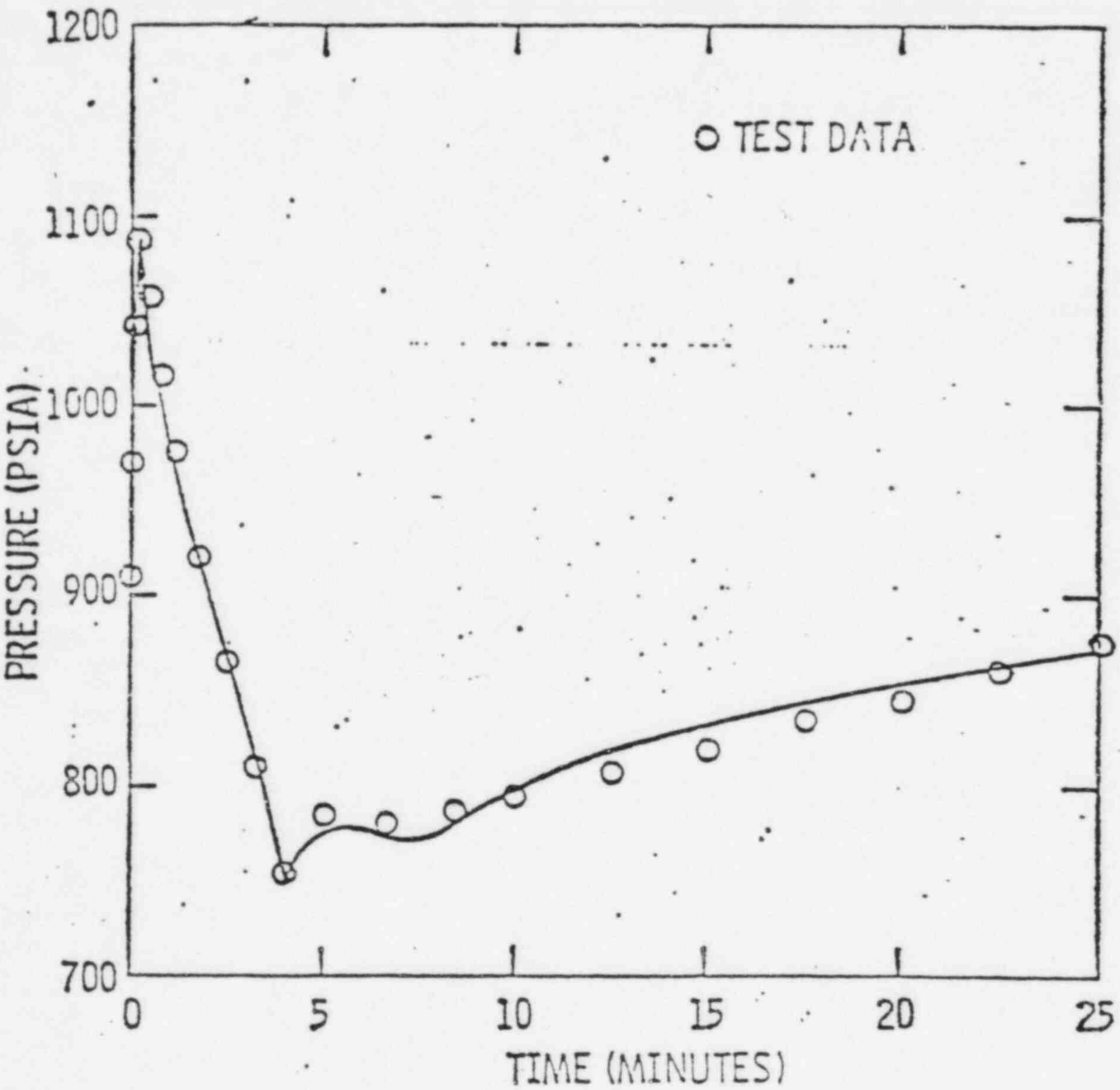

TURBINE TRIP FROM 100% POWER (LONG TERM RESPONSE)
STEAM GENERATOR B PRESSURE

FIGURE V-1
PROCESS MODEL STRUCTURE
AND PRINCIPAL INTERFACES

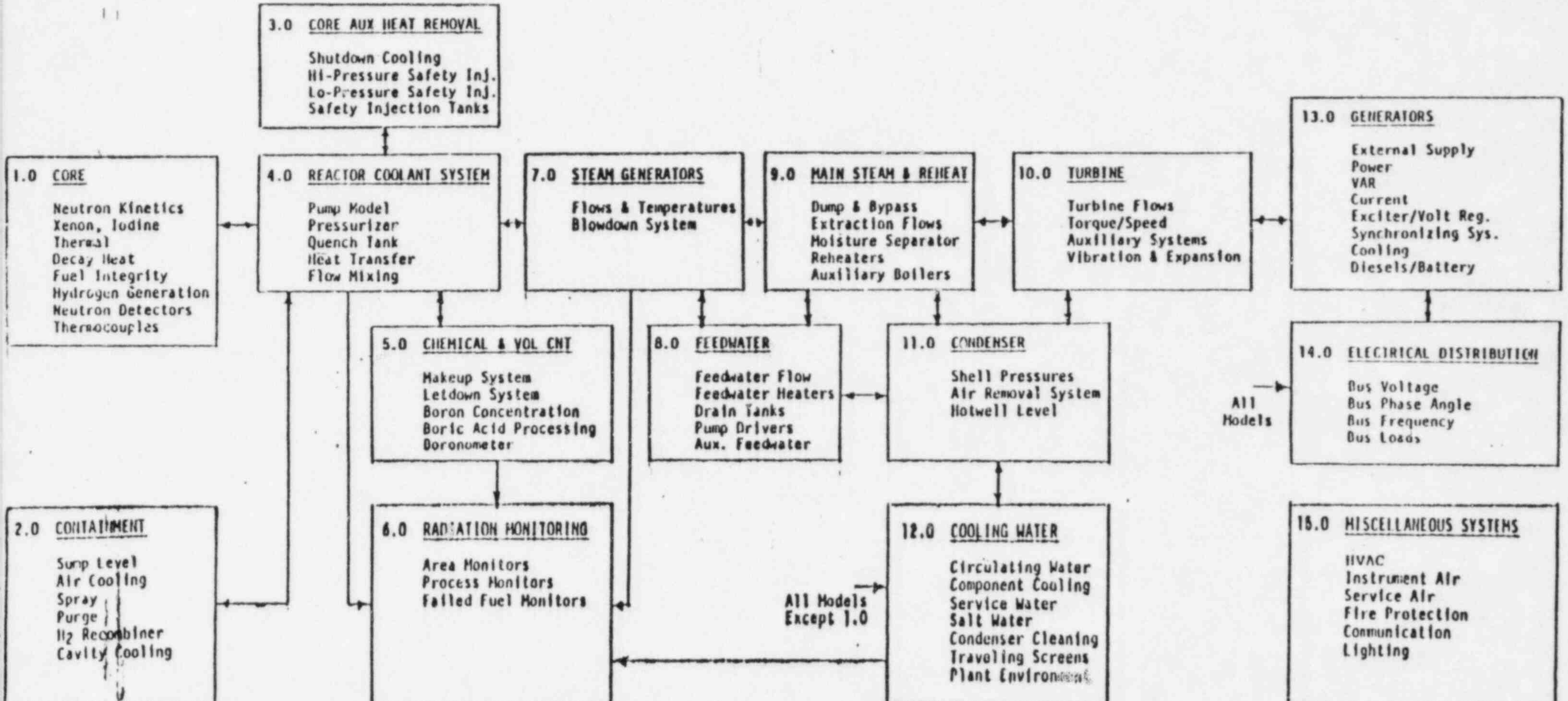

FIGURE V-2
CONTROLS MODEL STRUCTURE
AND PRINCIPAL INTERFACES

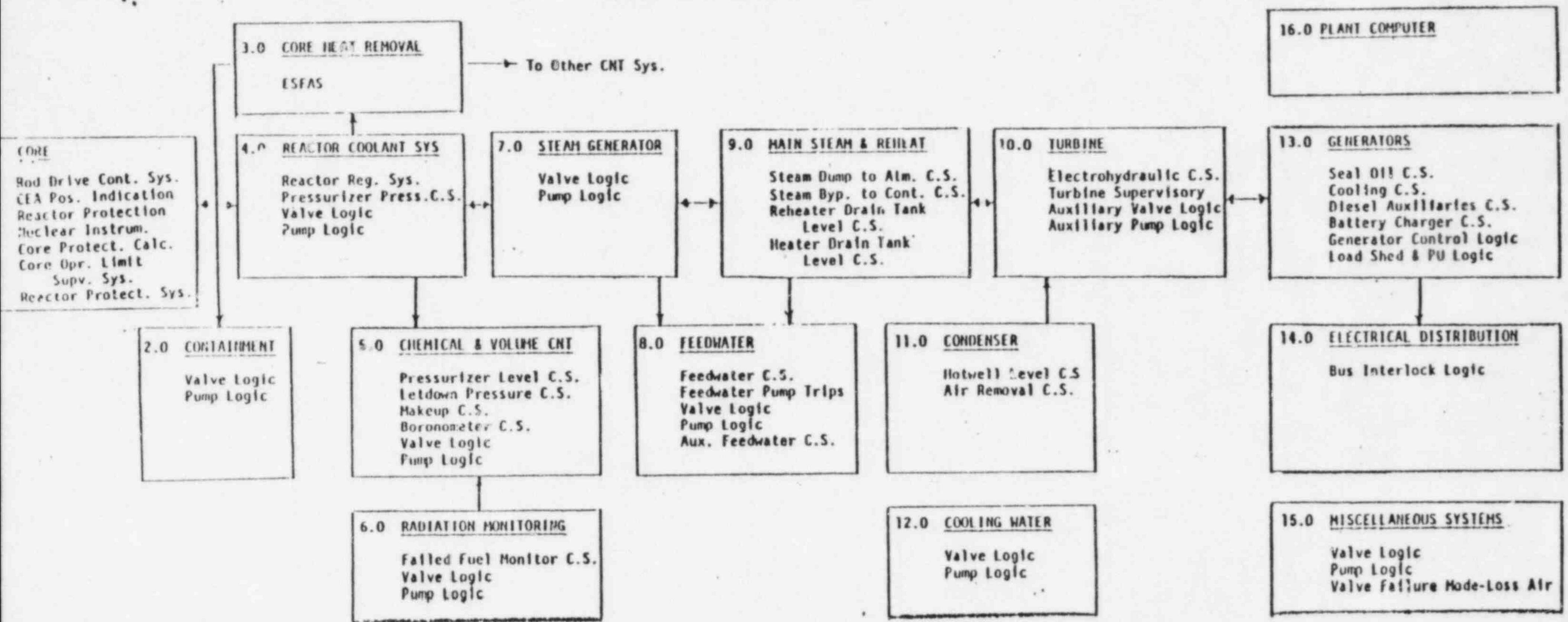

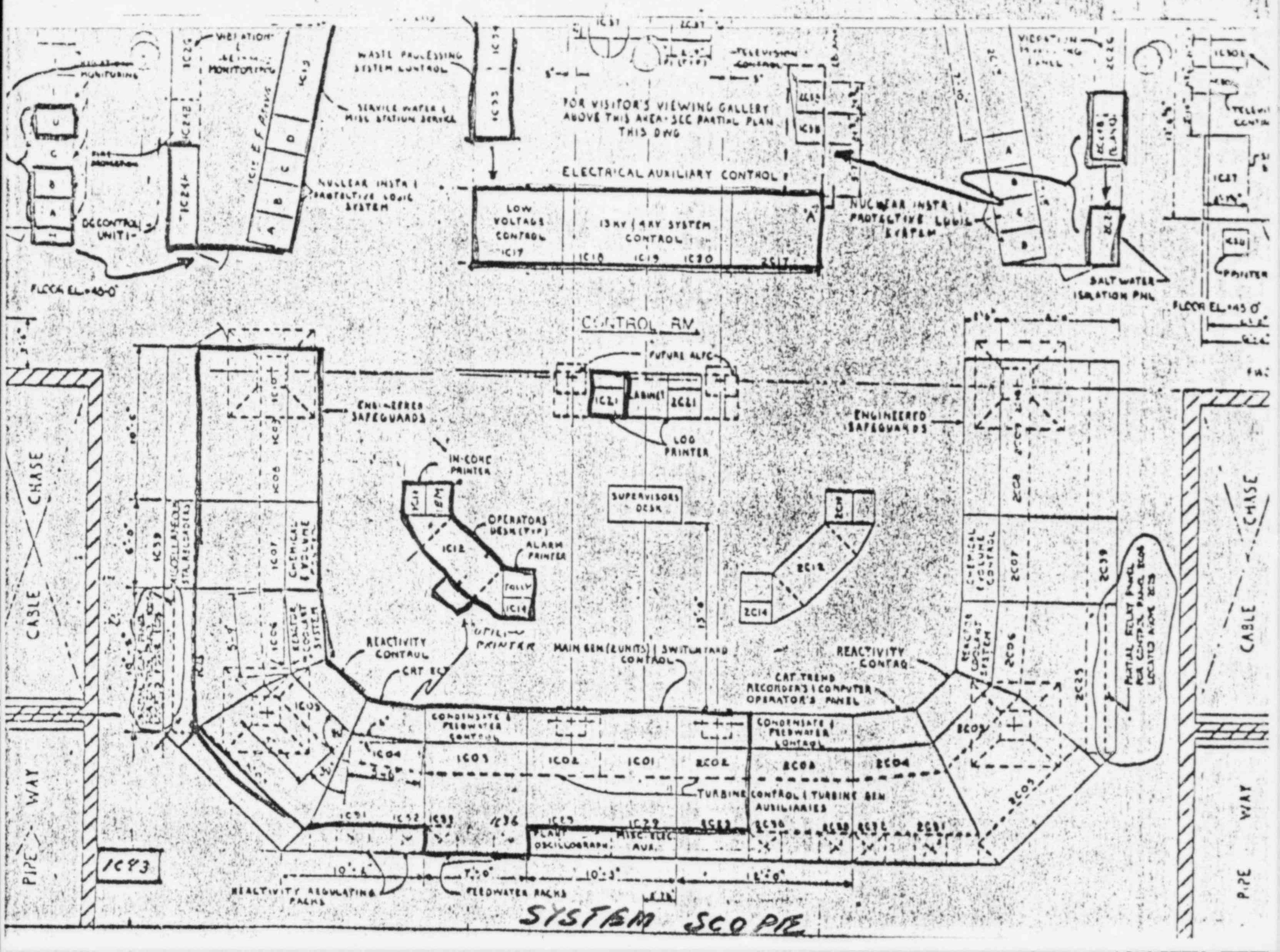

FOR VISITOR'S VIEWING GALLERY ABOVE THIS AREA - SEE PARTIAL PLAN THIS DWG
ELECTRICAL AUXILIARY CONTROL
LOW VOLTAGE CONTROL
1C17
13 KV / 4 KV SYSTEM CONTROL
1C18
1C19
1C20
2C17
WASTE PROCESSING SYSTEM CONTROL
SERVICE WATER & MISC STATION SERVICE
NUCLEAR INSTR & PROTECTIVE LOGIC SYSTEM
MONITORING
DECONTROL UNIT
FLOOR EL +45-0"
SALT WATER ISOLATION PNL
PRINTER
CONTROL RM
FUTURE ALPC
LOG PRINTER
1C21
CABINET
2C21
ENGINEERED SAFEGUARDS
IN-CORE PRINTER
OPERATORS DESK (TYP)
ALARM PRINTER
1C12
1C14
2C12
2C14
UTILITY PRINTER
SUPERVISORS DESK
MAIN GEN (2 UNITS) & SWITCHYARD CONTROL
REACTIVITY CONTROL
CRT EC
CRT TREND RECORDERS & COMPUTER OPERATOR'S PANEL
CHEMICAL & VOLUME CONTROL
REACTOR COOLANT SYSTEM
MISCELLANEOUS STR RECORDERS
1C39
1C07
1C06
1C05
1C08
1C09
2C39
2C07
2C06
2C05
2C08
2C09
2C25
PARTIAL RELAY PANEL FOR CONTROL PANEL 2C06 LOCATED ABOVE 2C25
CONDENSATE & FEEDWATER CONTROL
1C04
1C03
1C02
1C01
2C02
2C03
2C04
TURBINE CONTROL & TURBINE GEN AUXILIARIES
1C31
1C32
1C33
1C36
1C23
1C22
1C43
PLANT OSCILLOGRAPH
MISC ELEC AUX.
REACTIVITY REGULATING RACKS
FEEDWATER RACKS
CABLE
CHASE
PIPE
WAY
SYSTEM SCOPE

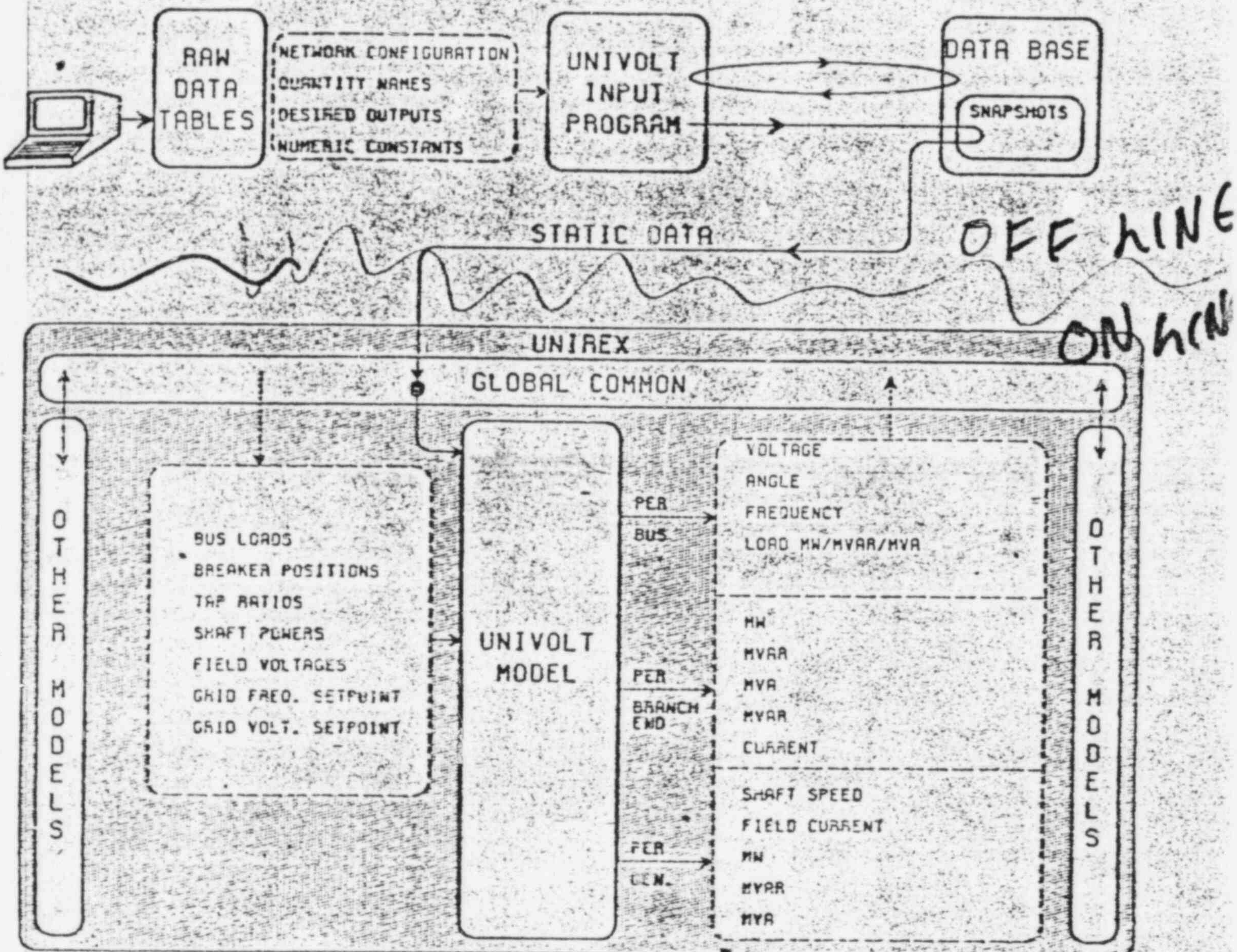

UNIVOLT AS A BLACK BOX
Figure 1

COMPREHENSIVE SYSTEM SIMULATION

PANEL/SYSTEM SCOPE

MODEL SCOPE

UNIFLOW

UNIVOLT - SYSTEM INTERACTION

POWER SUPPLY EFFECTS

COMPRESSED AIR

LOSS OF THE VITAL BUS 120V #12

CAUSE: SHORT OF 120V VITAL INSTRUMENT BUS #12

COMPONENT DESCRIPTION	BREAKER DESIGNATION	INITIAL POSITION	SIMULATOR RESPONSE
RCS Channels TR-125, TIC-121Y P/S X-7 (1C06)	1Y02-1	closed	loss of indication and control; Alarm
PZR Pressure Channels PY-102B and P/S X-22 (1C25B)	1Y02-2	closed	Relay Tripped; Alarm
Diesel Gen. 4KV Manual Disc. SW Indicator (1C18)	1Y02-3	closed	loss of indication
PZR Pressure Channel PIA-102B (1C06)	1Y02-4	closed	loss of indication; Alarm
RCS Loop Temp. Channels T-112B, T-122B P/S X-3, X-53, X-54, X-55 (1C25B)	1Y02-5	closed	loss of indication; Alarm
PZR Pressure Channels PY-100Y, PC-100Y, PIC 100Y, PA-100Y and P/S X-26 (1C06)	1Y02-6	closed	relays tripped, loss of control; Alarm
PZR Level Channels LC-110YL, LA-110YH, LC-110YH, LA-110YL, LIC-110Y, LY-101Y (1C06)	1Y02-7	closed	relays tripped, loss of control; Alarm
SG #12 FW Regulating System (1C36)	1Y02-8	closed	Automatic control trips feedwater control fails as-is
SG Level Channels LIC-1113B, LIC-1123B P/S X-15, X-63 (1C25B)	1Y02-9	closed	loss of indication and control, Alarm
RC Flow Channels F-101B P/S X-29 (1C25B)	1Y02-10	closed	loss of indication. Alarm
ESFAS (1C92)	1Y02-11	closed	tripped sensor channel annunciation

UNIVOLT
AND
UNIFLOW

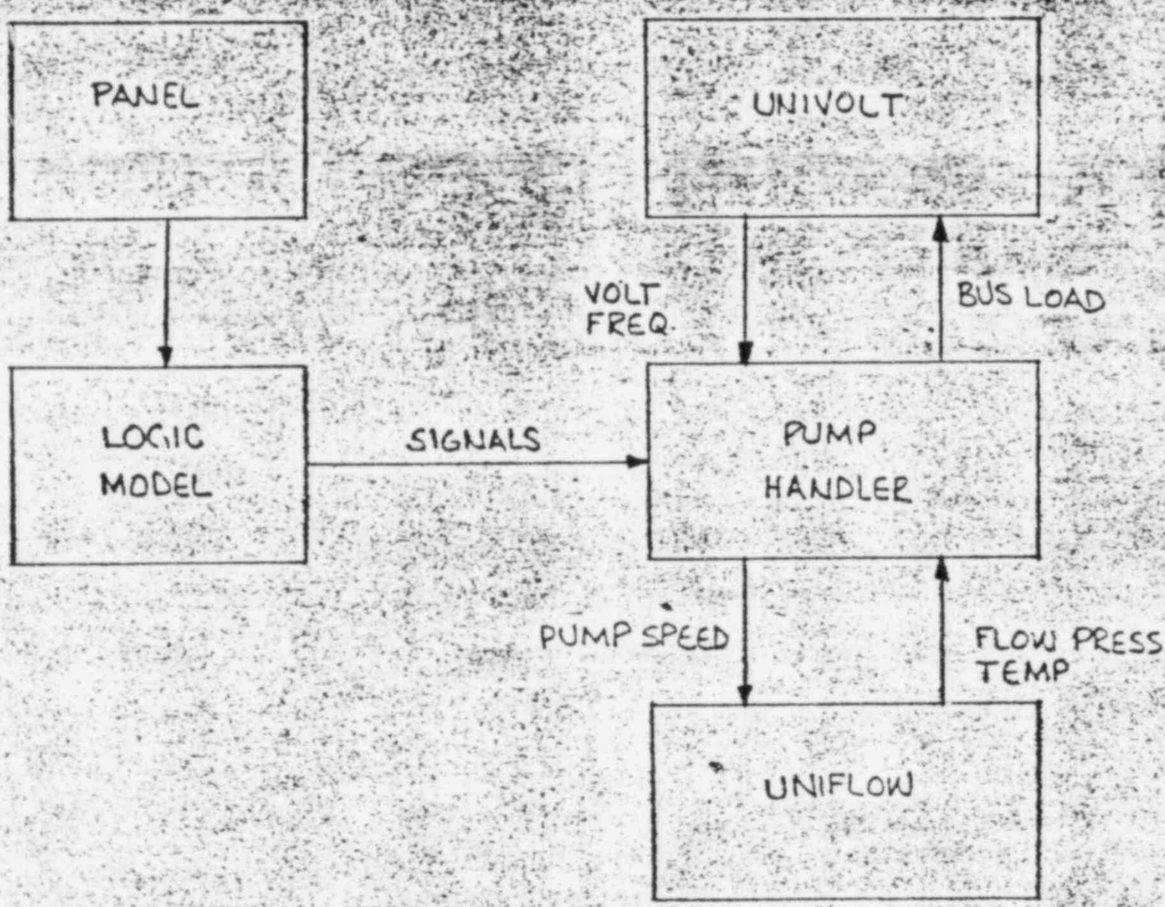

Figure V 3

ELECTRICAL AND PROCESS MODEL OVERVIEW

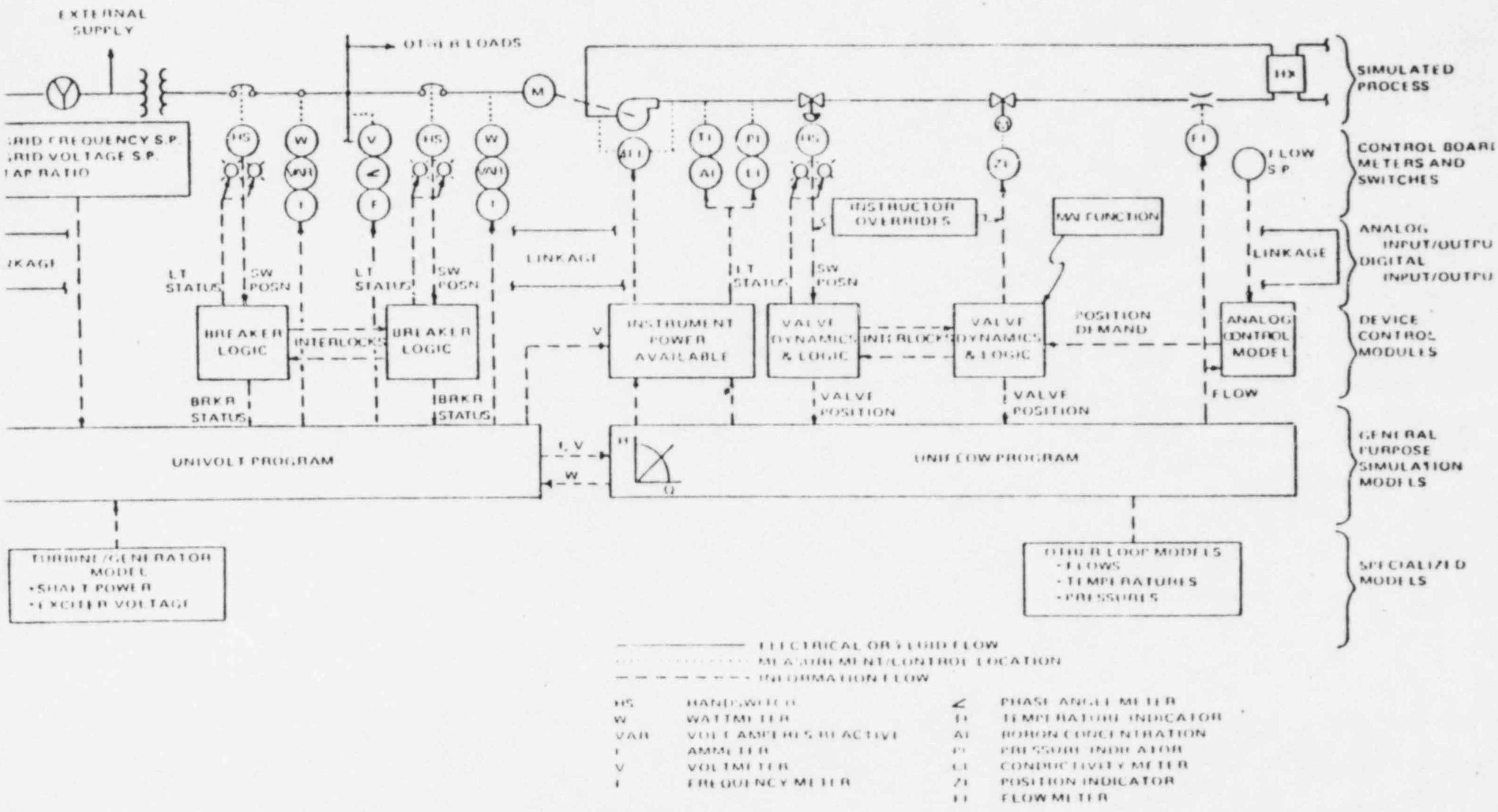

TABLE IV-1

Typical Simulation Program Characteristics

ogram ection	System	Development Basis	Classification (1)	Status (2)	Language	CPU Memory Reqd (3)	Exec. Time sec/sec	Frequency x/sec (4)	% CPU Use	Ass. CPU
1.0	Core	Flare Modified	C	1972/1983	Fortran	300KB	0.07	1,5,10/sec	25%	1
2.0	Containment	Contempt Modified	C	1968/1983	Fortran	100KB	0.01	2/sec	2%	2
3.0	Core Aux. HT Rem.	CESEC Modified	C	1970/1983	Fortran	100KB	0.03	5/sec	15%	2
4.0	Reactor Clnt. Sys.	CESEC/COAST Modif.	C	1970/1983	Fortran	260KB	0.02	5,10/sec	18%	1
5.0	CVCS	CESEC Modified	C	1970/1983	Fortran	50KB	0.01	2/sec	2%	2
6.0	Radiation Mon.	New & Uniflow	B	1983	Fortran	40KB	0.01	1/sec	1%	2
7.0	Steam Generator	Zambo Modified	C	1970/1983	Fortran	200KB	0.03	5/sec	15%	1
8.0	Condensate & Fdwtr.	Zambo Modified	C	1970/1983	Fortran	50KB	0.01	1,5,10/sec	6%	2
9.0	Main Steam & RH	Zambo Modified	C	1970/1983	Fortran	50KB	0.01	1,5/sec	4%	2
10.0	Turbine	Zambo Modified	C	1971/1983	Fortran	100KB	0.02	5/sec	10%	2
11.0	Condenser	Zambo Modified	C	1971/1983	Fortran	60KB	0.01	1/sec	1%	2
12.0	Cooling Water	Uniflow	C	1978/1983	Fortran	60KB	0.01	1/sec	1%	2
13.0	Generator	New	B	1983	Fortran	190KB	0.01	5/sec	5%	2
14.0	Electrical Dist.	Univolt	C	1977/1983	Fortran	100KB	0.015	5/sec	8%	2
15.0	Misc. Systems	Uniflow	C	1978/1983	Fortran	160KB	0.02	1,5/sec	3%	2
16.0	Plant Computer	Prodac Programs	C	1972/1983	Fortran	200KB	0.2	1/sec	20%	3

(1) Classification Key
- A - Standard Existing Software
- B - New Standard Software, to be developed
- C - Standard Software Modified for BG&E
- D - New Specially Designed Software for BG&E

(2) First date is initial use at C-E/second date is availability in a simulator system

(3) There is no auxiliary memory required nor is there an auxiliary memory transfer time

(4) I/O is capable of scan/update at 10 times per second

CC SIMULATOR

INHERENT CAPABILITIES

I/O

MALFUNCTIONS

REMOTES

EXTERNALS

MULTIPLE COMPONENTS:

GLOBAL NAME	COMPONENT
ISMAL_153(1)	BUS 11(2A)
ISMAL_153(2)	BUS 12(A)
ISMAL_153(3)	BUS 13(B)
ISMAL_153(4)	BUS 14(2B)
ISMAL_153(5)	BUS 15(A)
ISMAL_153(6)	BUS 16(A)

DOCUMENTED IN: MODEL SPEC MSC-013
SUBSYSTEM V4K

MALF 154 -- LOSS OF 480V UNIT BUS DUE TO SHORT OF BUS TO GROUND.

VARIABLE NAME: ISMAL_154   VARIABLE TYPE: LOGICAL*1   DIMENSIONED (9)

VALUES: .TRUE. - MALFUNCTION ACTIVE   .FALSE. - MALFUNCTION INACTIVE

MULTIPLE COMPONENTS:

GLOBAL NAME	COMPONENT
ISMAL_154(1)	BUS 11A(2A)
ISMAL_154(2)	BUS 11B(2A)
ISMAL_154(3)	BUS 12A
ISMAL_154(4)	BUS 12B
ISMAL_154(5)	BUS 13A
ISMAL_154(6)	BUS 13B
ISMAL_154(7)	BUS 14A(2B)
ISMAL_154(8)	BUS 14B(2B)
ISMAL_154(9)	BUS 15(A)

DOCUMENTED IN: MODEL SPEC MSC-013
SUBSYSTEM V480

MALF 155 -- LOSS OF REACTOR (480V) MCC DUE TO SHORT OF BUS TO GROUND.

VARIABLE NAME: ISMAL_155   VARIABLE TYPE: LOGICAL*1   DIMENSIONED (4)

VALUES: .TRUE. - MALFUNCTION ACTIVE   .FALSE. - MALFUNCTION INACTIVE

MULTIPLE COMPONENTS:

GLOBAL NAME	COMPONENT
ISMAL_155(1)	BUS 104R(2B)
ISMAL_155(2)	BUS 114R(2A)
ISMAL_155(3)	BUS 105R
ISMAL_155(4)	BUS 115R

DOCUMENTED IN: MODEL SPEC MSC-013
SUBSYSTEM MCC

PROCEEDINGS OF
THE FIFTH POWER PLANT DYNAMICS, CONTROL AND TESTING SYMPOSIUM

•

March 21-23, 1983
Knoxville, Tennessee

Edited by
B.R. UPADHYAYA

VOL. 1 OF 2

SPONSORED BY

THE UNIVERSITY OF TENNESSEE, KNOXVILLE
COLLEGE OF ENGINEERING

•

COOPERATING ORGANIZATIONS

AMERICAN NUCLEAR SOCIETY
IEEE CONTROL SYSTEMS SOCIETY
ELECTRIC POWER RESEARCH INSTITUTE

•

DEPARTMENT OF NUCLEAR ENGINEERING
THE UNIVERSITY OF TENNESSEE, KNOXVILLE, TENNESSEE

THE UNIVERSITY OF TENNESSEE
1794

APPLICATION OF THERMAL-HYDRAULIC DESIGN CODES TO REAL TIME PWR SIMULATION

R. J. Espinosa, P. K. Doherty, R. L. McBeth

Nuclear Power Systems
Combustion Engineering, Inc.
Windsor, Connecticut

SUMMARY

Improved thermal-hydraulic models for real time reactor simulation are described. They are based on models used in reactor design codes. The primary system model is formulated with five one-dimensional continuity equations conserving liquid and steam mass, liquid and steam energy and momentum. The models incorporate two-phase, nonhomogeneous, nonequilibrium capabilities based on first principle physics. Validation of the design codes by reactor test data is described. The ability of the models to predict proper system behavior is demonstrated for a pump transient, an overcooling transient, and a small break loss of coolant accident (LOCA).

The feasibility of developing and integrating models for the primary and secondary system which execute faster than real time on computers used in simulators is shown. The resulting simulator thermal-hydraulic models can directly calculate plant response for a wide range of normal and abnormal conditions including LOCAs. Full provision for operator intervention or multiple failure interactions is available. Reality of plant behavior is maintained and the capability to perform calculations in support of design studies and development of operating procedures is provided.

INTRODUCTION

Presentations given at the conference on Simulation Methods for Nuclear Power Systems held two years ago highlight limitations of the power reactor simulators in use at that time[1]. The models are limited to a single-phase fluid representation. Phase-separation and nonequilibrium effects are not represented. As a consequence, the more severe transient responses are often preprogrammed. Operator interaction with preprogrammed transients is not possible. Unrealistic responses are obtained in many cases with a possibility of resultant inefficient training of the operator.

Since the Three Mile Island Unit 2 (TMI) accident in March 1979, new capabilities have been defined for power reactor simulators. The ANS 3.5 Standard lists a number of the required capabilities including normal plant evolutions and abnormal conditions resulting from malfunctions[2]. The post-TMI NRC Action Plan lists additional requirements particularly in the Reactor Coolant System (RCS) Models[3]. Among the currently required capabilities are the following. Operator interaction with the transient is needed where operator actions can influence the severity of the malfunction. The simulation must continue until a stable, safe and controllable condition is attained which can be continued to cold shutdown conditions. Observable control room indications must be realistic to provide proper training of the operator. Multiple failures or malfunctions must be modeled with appropriate interactions. An additional desired feature is the ability to do engineering calculations to support design studies and development of operating procedures.

Satisfaction of these requirements demands addition of new first-principle physics models. Most important is the addition of two-phase modeling capability for saturation conditions which occur in natural circulation cooldown as well as the more severe transients such as a small break LOCA. The stuck open pilot operated relief valve (PORV) at TMI produced a small break LOCA transient. Such a transient requires phase separation capability and nonequilibrium models to provide realistic pressure transients when fluids of very different temperatures interact. Real time simulation is required, so very efficient algorithms are needed.

Existing thermal-hydraulic system design and accident analysis codes provide the desired physical models. They are routinely used to analyze a full range of thermal-hydraulic transients including accidents leading to two-phase fluid conditions. However, these codes have been of limited use in training simulators since the computers used in simulators cannot provide the required computational speed to maintain real time simulation. The design codes also lack the detailed representation of system hardware required to drive the simulator control panel. The problem then is to combine the more complete physical models of the design codes with the real time requirements of a simulator.

COMBUSTION ENGINEERING SIMULATOR

Combustion Engineering is currently building a full scope control room training simulator for a Pressurized Water Reactor (PWR). The simulator models the complete PWR -- core, primary system, secondary system, turbo-generator, balance of plant, control systems, control panel, plant computer and instrumentation. It is capable of simulating plant behavior in real time during normal and abnormal operation. It simulates the dynamic response of the power plant to operator actions and system malfunctions activated by the instructor. It is designed to be utilized as a training device, as a tool for development and verification of new operating procedures, and as a tool for plant improvement studies.

Modeling of the Nuclear Steam Supply System (NSSS) is based on state-of-the-art design codes used for design and analysis of the major NSSS components and systems. The design codes have been verified with respect to PWR plant response data, to integral test facilities such as the Loss of Fluid Test (LOFT) facility or to separate effects tests. Additional models are provided for balance of plant systems.

The simulator uses computer hardware with proven performance and reliability. A Perkin-Elmer model 3244 computer in a four computer multiprocessor, shared memory configuration is used. This supplies the required computational capability with provision for support of related computational needs. Final code is in FORTRAN 77 compatible with the ANSI Standard. A unified software package manages the computer resources, includes generalized solution packages for balance of plant systems, and provides consistent software standards for coding of models.

The control panels closely parallel the panels of the reference plant. They include the full range of control, indicating and annunciating devices found in the power plant. An instructor's panel is also included to run the simulator and activate malfunctions during operator training. Over 200 malfunctions are provided for the instructor.

THERMAL-HYDRAULIC MODEL DESCRIPTION

The C-E Full Scope Simulator is designed to provide realistic thermal-hydraulic responses and instrument indications for a full range of reactor operating conditions. The models are based on those found in computer codes used for PWR design. The primary system or Reactor Coolant System (RCS) models are based on those used in a best estimate, design version of the CEFLASH-4AS computer code[4]. This code provides realistic RCS responses for a full range of system conditions including a loss of coolant accident. The secondary system models are taken from the Long Term Cooling (LTC) computer code[5]. The code is used to evaluate the integrated plant response to operational and accident conditions. Highlights of the more important models are given here.

Primary System Geometric Representation

The primary system thermal-hydraulic response is modeled by a node and flowpath network. The nodes enclose control volumes which represent the fluid mass and energy. Flowpaths connecting the nodes represent the fluid momentum and have no volume. The separation of mass and energy into control volumes and momentum into flowpaths is similar in concept to that used in the FLASH-4 code[6].

The simulator geometric representation for a typical C-E PWR (for all conditions but a large break LOCA) is shown in Figure 1. Nodes are provided for the major components in the reactor primary system — inner vessel, upper head, control element assembly guidetubes, two hot legs (including the associated steam generator inlet plenum), a pressurizer, two steam generators (separate hot and cold sides of the U-tubes), two combined outlet plenum and suction legs, four cold legs and reactor coolant pumps, and the annulus or downcomer for the reactor vessel. A total of 17 control volume nodes are used in the RCS model. The separate cold leg representations provide appropriate responses for partial loop operation. The interface with the secondary system occurs at the steam generator tube bundle.

More than 20 flowpaths with momentum solutions are used in the RCS model. Separated counter-current flow is represented in the hot and cold legs. An additional 32 non-momentum flow paths are provided for addition and removal of coolant from the RCS by the emergency core cooling system (ECCS), pressurizer spray, charging pumps, letdown system, shutdown cooling system, and safety and relief valves.

The noding and flowpath modeling detail is not hardwired. The detail in representation of the system can be changed through input during the modeling process to tailor the representation to the requirements of a particular PWR design. Geometric features such as the number of loops or the number of steam generators as well as geometric details such as node volume, elevations, piping resistance, etcetera, are specified in a data base. Adoption of the RCS models for another plant does not require extensive recoding of the software as is done in earlier simulators.

Conservation Equations

The RCS thermal-hydraulic model is formulated with five one-dimensional continuity equations. The conservation variables are mixture (liquid and steam) mass, liquid mass, mixture energy, steam energy, and mixture momentum. The mass and energy for the liquid and steam are calculated for each node. Mass flowrate is calculated for each flowpath. The code incorporates slip effects in the flowpaths by means of empirical correlations[7].

The conservation equations are integrated implicitly by means of a simultaneous solution of the linearized, discretized conservation equations. This yields a (4xM+N) by (4xM+N) system of linear equations, where M is the number of nodes and N is the number of momentum flowpaths. The structure of the coefficient matrix permits use of a system reduction procedure which produces a NxN system of equations. The NxN matrix is solved using a block inversion technique[8].

After solution of the conservation equations, the pressure in each node is calculated. The mass and energy in the liquid and steam regions are used with the water property correlations and nodal volume to determine the resulting state variables (pressure, phase enthalpies and phase temperatures).

Two-Phase Fluid Representation

The simulator models phase separation within a node into a separate steam region and a liquid or two-phase region consisting of a continuous liquid phase with dispersed bubbles. Bubbles are generated by heat sources within the node, flashing in the node or transport from the adjacent nodes. Phase separation is calculated in terms of bubble rise velocities which are found from experimentally based drift flux correlations[9]. A more detailed model provides an axial bubble mass distribution in the inner vessel node[10]. Nodes with phase separation provide a discrete two-phase mixture level in the node. Fluid level effects on heat transfer and the quality of fluid exiting through flowpaths connected to the node are modeled.

Nonequilibrium States

The simulator provides a full range of thermodynamic fluid states for all nodes. Nodes with homogeneous or fully mixed fluid are at equilibrium. States for nonhomogeneous or phase separated nodes with separate two-phase mixture and steam regions are subcooled liquid-saturated steam, saturated liquid-superheated steam, and subcooled liquid-superheated steam. The model dynamically calculates the node thermodynamic state. It includes a detailed flow regime dependent condensation model which considers condensation of bubbles, vapor condensation on an injected subcooled liquid, condensation at the surface of a liquid pool, and vaporization due to wall heat. In addition, energy partitioning of wall heat transfer between the liquid (two-phase) and steam regions is calculated.

Reactor Core

Reactor power is calculated, by a three-dimensional reactor core model described in these proceedings[11]. An axial power distribution and radial power tilt are taken from the reactor core model. Axially varying heat transfer and core coolant data is provided to the core model to provide a full range of temperature and moderator driven feedbacks.

The core heat transfer model covers the full range of fluid conditions in the core. Provision is made for forced convection and quiescent pool boiling conditions. The mode of heat transfer is determined dynamically. Boiling curves for both conditions include subcooled, nucleate boiling, transition boiling, film boiling, and steam heat transfer correlations. Fuel temperature, cladding temperature, and the heat flux, hence, the heat transfer regime and surface heat transfer coefficients, are calculated implicitly. Appropriate radial noding detail is used in the fuel rods. The axial nodal detail is varied depending on whether forced convection or pool boiling is occurring.

Other Primary System Models

The simulator models all primary system components. Some additional models of interest are discussed here. Reactor coolant pump (RCP) performance is found by conservation of angular momentum and homologous curves for single- and two-phase conditions with two-phase head degradation. Wall heat transfer, pressurizer heaters, and pump heat are modeled. Coolant inventory changes due to systems such as charging pumps, the emergency core cooling system, the chemical volume control system, and auxiliary pressurizer spray are calculated using a general purpose, single-phase flow solution software package. Critical flow out of the primary system, through leaks or relief valves, is found from standard critical flow correlations[12]. Generation of non-condensible gases and their collection in the upper head are modeled. Coolant thermodynamic properties are found from a set of fast water property correlations specially designed to provide continuous property derivatives for a full range of fluid conditions -- subcooled, saturated, and superheated.

Steam Generator Heat Transfer

Models for forward and reverse heat transfer are incorporated in the steam generator heat transfer logic. The overall heat transfer is determined from film resistence of the primary and secondary sides and the wall resistance. The primary side film resistance for forward heat transfer is found from correlations for subcooled forced convection and two-phase condensation. The primary side reverse heat transfer is found from correlations for nucleate boiling and heat transfer to steam. The secondary side film resistance is calculated using pool boiling and heat transfer to steam correlations. Fluid level is modeled on both the primary and secondary side of each steam generator. The effect of fluid level on heat transfer area is modeled on both sides.

Steam Generator Secondary System Geometric Modeling

For a plant with two steam generators, the steam generator secondary system is represented by a seven node model, Figure 2. Three nodes are used for the secondary side of each steam generator — a downcomer (saturated or subcooled), an evaporator region (saturated or subcooled), and a steam drum (saturated or superheated). One additional node represents the common steam line header. This system representation allows accurate modeling of the recirculation phenomena and the downcomer and evaporator water levels. In addition, by collapsing nodes, the model can represent dry steam generators. All major components are modeled, including the secondary safety valves, atmospheric dump valves, and main steam isolation valves. All main steam flow paths are considered.

Secondary System Conservation Equations

Mass and energy balances are made for each node. The flow between the downcomer and the evaporator, and the main steam flows are calculated using momentum balances. The recirculation flow from the evaporator to the steam drum is calculated using a bubble rise model. The pressure and remaining state properties are calculated from the mass and energy in each node.

REAL TIME CAPABILITIES OF THERMAL-HYDRAULIC MODELS

An important consideration in the selection of the thermal-hydraulic models for the simulator was the ability to obtain a faster than real time calculational speed. The design code thermal-hydraulic models selected as a basis for the primary and secondary systems generally run much faster than real time on a high speed computer such as the CDC 7600. However, the Perkin-Elmer 3244 computer used in the C-E simulator would not provide the needed calculational speed for the design code RCS models. Two classes of changes were made to the primary system design code models to satisfy the real time computational requirement -- model optimization and model changes allowing use of long and constant time steps. Code optimization provided substantial time savings. An example is the water property package. Use of high speed polynomial fits, less frequent evaluation of properties which change slowly, and linearization of properties reduced the computational time to one-tenth that required formerly. Also, simplification of design code models reduced computational time. Removal of options and detailed models particular to design calculations, which are not required for the simulator, provided the needed simplification.

Use of a constant time step length allows the simulator thermal-hydraulic models to keep up with real time. It requires accommodation of potential discontinuous transitions which would produce abrupt changes observable by the operator or even instability with constant time steps. An example is addition, in a single time step, of more liquid to a node than the available steam volume can hold. This overfilling, or node packing phenomenon, produces a severe pressure spike. Use of an approximate solution technique provides smooth pressure results until normal conditions are obtained. A similar technique applies to overdraining a node, removing more water in a time step than was present. Linearization of other equations describing transitions also allows elimination of discontinuous behavior. Use of more implicit mathematical representations was also needed for some models. Fully implicit modeling of the core heat transfer, bubble release calculations, and pump speed calculations allows use of much longer time step lengths. Use of larger nodes also reduces calculational time by increasing the permissible time step length. Some temporal detail is lost with little effect on the information seen by the operator. The model performance is fully satisfactory.

Less geometric detail in the primary system noding and flowpaths is used for the large break LOCA calculation. The RCS time step length is reduced. No change is made in the secondary side model. This allows direct calculation of a large break LOCA in real time.

The computational speed of the thermal-hydraulic models has been tested by running a wide range of operational simulations from steady state through accidents with two-phase fluid conditions. The computational speed results are shown in Table 1. The combined time for the primary and secondary thermal-hydraulic models is much faster than real time, providing the desired overall real time capability for the simulator. The same constant time step is used for both the primary and secondary system models.

Table 1

Computational Time for Thermal-Hydraulic Models*

	Primary	Secondary
Perkin-Elmer 3244	250	40
CDC 7600	20	--

*Computational time in milliseconds per second of real time.

MODEL VALIDATION

Validation of the design codes upon which the simulator models are based is obtained, in part, by comparison of analyses of experimental transients and data from experiments. The best estimate version of the CEFLASH-4AS code has been extensively tested by such comparisons for both separate effects tests and integral tests on both the Semiscale and LOFT facilities. Two integral system test comparisons are shown for CEFLASH-4AS. The design code used as a basis for the secondary system models has been tested with separate effects data and with power plant performance data. One power plant transient is shown for this code.

LOFT test L3-1 simulated a 0.09 square foot single ended pump discharge break, a small break LOCA, for a full size PWR. A comparison of the system behavior calculated with the best estimate CEFLASH-4AS code and experimental results is shown in Figure 3[13]. The agreement between the data and the prediction is excellent. The predicted time of accumulator actuation is almost exact and the predicted behavior of the reactor vessel two-phase mixture height before and after accumulator actuation is very similar to the data. Predicted accumulator discharge does not result in a rapid depressurization and a high accumulator flow rate as normally occurs with thermal equilibrium codes.

Confirmation of the ability of the CEFLASH-4AS code to represent reactor behavior for a two-phase transient with the reactor coolant pumps (RCP) running is provided by the LOFT L3-6 test[14]. This test simulated a 0.1 square foot cold leg small break LOCA with the RCP powered throughout the transient. Figures 4 and 5 compare best estimate CEFLASH-4AS calculations with the test results. The analysis predicts the primary pressure, Figure 4, quite accurately. Reasonable agreement is provided for the primary system inventory, Figure 5. The homogeneous and nonhomogeneous or separated flow regimes agree very well with gamma densitometer data from the test. These results and those for the LOFT L3-1 test demonstrate the ability of the CEFLASH-4AS best estimate code to accurately model reactor thermal-hydraulic behavior during severe transients such as a small break LOCA. The next section demonstrates a comparable calculational capability for the simulator.

Comparisons of nuclear plant calculations made by the code upon which the secondary system models are based, with experimental results, are presented in Reference 15. Power plant test data including step changes in power, plant trips, and reactor coolant pump trips are discussed. A plant cooldown transient under natural circulation conditions and an overcooling transient are included. The design code is shown to be valid for a variety of events of interest. A high degree of correlation between the analytical predictions and the test data is shown to exist. Results for the overcooling transient, found with the simulator model, are presented in the next section.

PERFORMANCE OF SIMULATOR THERMAL-HYDRAULIC MODELS

The simulator thermal-hydraulic model performance has been evaluated for a wide range of PWR operation from normal plant evolutions to severe accidents. The accuracy of the steady state predictions is confirmed by their consistency, comparison to plant data, and comparison to design code calculations. The steady state calculations demonstrate correct implementation, proper interfacing, and numerical stability of the models. Operational transients are matched to plant performance or design code calculations. These include power changes and startup or shutdown of various devices including the RCPs, pressurizer sprays or heaters, and inventory control systems such as the ECCS systems. Many of the abnormal or accident transients normally can only be compared to design code analyses. Representative accident transients are small and large break LOCAs, steam-line breaks, loss of feedwater, and anticipated transients without scram. Appropriate behavior for these transients is necessary to provide optimal operator training.

Three examples of the testing program are shown here. The first is a single-phase RCP transient including steady state conditions and a series of abrupt changes in RCP operation. Next is an overcooling transient. Last, is a small break LOCA including an extended period with two-phase conditions, core uncovery, and initiation of core recovery. The test cases were run with the simulator thermal-hydraulics software on the Perkin-Elmer 3244 computer. All cases were run with real time computational speeds similar to those shown in Table 1.

Single-Phase Reactor Coolant Pump Transient

The RCP transient is designed to show proper steady state operation and to demonstrate the thermal-hydraulic model's response to abrupt change in single-phase coolant flow. It begins at full power. Next the core is scrammed and the RCPs and turbine are tripped. This is followed by restart of each RCP singly, and shutdown of two pumps. The transient is summarized in Table 2.

Table 2

Reactor Coolant Pump Transient Event Summary

Time (Seconds)	Event
0	Start steady state at full power
50	Scram reactor, trip all RCPs, trip turbine.
100	Restart Pump 1*
150	Restart Pump 2
200	Restart Pump 3
250	Restart Pump 4
300	Trip Pumps 2 and 3
350	End of transient

*Pump numbers are shown on Figure 1.

Figures 6 and 7 show the pressurizer pressure and level. Figures 8-11 show the flow rate through reactor coolant pumps 1-4, as designated in Figure 1. The system maintains a constant steady state for the first 50 seconds. No drift or oscillation is observed. Reactor scram and pump trip at 50 seconds is followed by pump coastdown. Pressurizer level drops throughout the transient due to inventory shrinkage by the coolant density rise. Charging pumps are not actuated as the pressurizer level drops.

The effect of restarting one pump every 50 seconds is shown in Figures 8-11. Coolant flow through each restarted pump rises abruptly. When pump 1 is restarted, flow through the tripped pumps rapidly becomes negative. As each additional pump is restarted, the flow through the previously operating pumps drops and the magnitude of the negative flow in the tripped pumps increases as expected. Trip of pumps 2 and 3 at 300 seconds rapidly produces the same flow rate in pumps 2 and 3, a negative flow, and in pumps 1 and 4, a positive flow. The path of the coolant flow can be traced in detail by referring to Figure 1. The coolant flows from pump 1 through the cold leg to the annulus. Part of the coolant goes through the core, hot leg and steam generator back to pump 1. The remainder goes back through the adjacent cold leg in reverse flow through pump 2 to the steam generator outlet plenum, and finally through pump 1 in forward flow. The same process is repeated for the components on the other side of the reactor vessel. The ability of the models to represent both symmetric and asymmetric flow distributions with both forward and reverse flow through the RCPs is demonstrated.

Overcooling Transient

A steam generator secondary system overcooling transient is used to illustrate the ability of the simulator thermal-hydraulic models to match measured PWR data. The pressurizer level and pressure, steam generator secondary pressure and level, and the hot and cold leg temperatures calculated by the simulator are compared to measured plant data[15]. The simulator calculation is done for a plant with a lower power level than the reference data plant. Some difference in plant behavior is expected due to differences in the plants, but a meaningful comparison is expected because the parameters controlling the transient were selected to produce the same key events and similar trends in plant behavior. The overcooling transient is initiated by a turbine trip from full power after which a steam bypass valve fails to close. The initiating events are summarized in Table 3. This is the same PWR transient discussed earlier in connection with validation of the steam generator secondary design code.

Table 3

Overcooling Transient Initiating Event Sequence

Time	Event
0	Turbine trip (manual)
1	Steam dump and bypass valves begin to open
6	Reactor trip (on low steam generator level)
18	Emergency feedwater to steam generators
21	One steam bypass valve fails to close
200	Reactor coolant pumps tripped (manual - on low primary pressure)
240	Main steam isolation valves closed (on low secondary pressure)
240	Main feedwater isolation valves closed
1200	Plant conditions stabilized

Following transient initiation by manual turbine trip the steam generator secondary pressure, Figure 12, rose rapidly until scram. Primary pressure also rose rapidly until scram, Figure 13. Steam generator level dropped after scram, Figure 14*. Pressurizer level rose initially until scram after which it fell, Figure 15. The simulation held one steam generator bypass valve open to

---

*Steam generator level is referenced to the level of the narrow range pressure tap.

represent the failure experienced in the PWR transient at 21 seconds. This initiated an overcooling event on the steam generator secondary side which caused the pressure and level to drop rapidly, Figures 12 and 14. The overcooling also caused the pressurizer pressure and level to drop rapidly, Figures 13 and 15. This portion of the transient provides a significant challenge to the simulator model's ability to calculate the compression and expansion experienced in the tests. The simulator reproduces the system behavior shown in the PWR test data.

Closure of the main steam isolation valves at 240 seconds ended the plant cooldown. After this, addition of emergency feedwater caused the steam generator secondary level and pressure to rise gradually. The rise in secondary temperature produced an increase in pressurizer pressure and level. Again the simulator reproduces the PWR transient during the pressure recovery. The thermal-hydraulic models successfully predict the significant events of the steam generator secondary pressure and water level dynamics. The nonequilibrium models and detailed momentum solution provide an appropriate prediction of the pressurizer pressure. The simulator successfully predicts the pressurizer water level indicating an adequate prediction of the RCS temperature history. Figure 16 shows this successful RCS temperature prediction capability for the hot leg and cold leg temperatures. Establishment of natural circulation and the resulting increase in core coolant temperature rise, after the RCPs are tripped, is demonstrated.

Small Break Loss of Coolant Accident

A small break LOCA transient is used to illustrate the simulator thermal-hydraulic model's ability to handle a severe accident. This transient is particularly challenging since the two-phase fluid conditions, core uncovery, core recovery, and emergency core cooling system cold water injection test the phase separation, nonhomogeneous and nonequilibrium models. The simulator analysis results are compared to those from a best estimate CEFLASH-4AS calculation. The significant initiating events for the transient are described in Table 4.

Table 4

Small Break LOCA Initiating Event Sequence

Time (Seconds)	Event
0	Open 0.12 ft^2 break in one cold leg
11	Scram core, trip turbine, trip RCP
50	Initiate HPSI
2500	End of transient

The small break LOCA is initiated by opening a 0.12 square foot break in one cold leg of the primary system. The major events and trends of the transient are summarized in Table 5. The best estimate and simulator primary pressure predictions are shown in Figure 17. The pressure drops rapidly for 80 seconds, plateaus with a moderate rise until 270 seconds, and drops gradually until 1500 seconds when it levels off. The inner vessel two-phase mixture level prediction by the best estimate code and the simulator are shown in Figure 18. The level drops rapidly until 70 seconds, pauses until 400 seconds, and falls gradually due to coolant boil-off until about 1200 seconds when core recovery begins. Core uncovery occurs at about 700 seconds. The core exit fluid temperature predicted by the simulator is shown in Figure 19 with the saturation temperature. The temperature is subcooled initially, stays at saturation until the core uncovers, rises to a peak and falls toward saturation shortly after core recovery begins.

Table 5

Small Break Transient History

Time (Seconds)	Discussion
0	LOCA initiated by opening 0.12 ft^2 cold leg break, rapid drop of inner vessel pressure and two-phase mixture level
20	Transition from subcooled to saturated blowdown
40	Pressurizer drained
70	Pause in inner vessel level change. Upper head and plenum drained, draining of steam generators and hot legs begins
80	Plateau in primary pressure just above secondary heat sink pressure
270	Pressure drop resumes upon transition to steam blowdown
400	Inner vessel level resumes gradual decline after draining higher elevation components
700	Core uncovery begins, temperature of core exit steam rises above saturation
1200	Minimum core level reached, refill begins
1500	Pressure stabilizes at 250 psia
1550	Core exit steam temperature peaks and soon begins a gradual decline

The simulator reproduces the small break LOCA behavior predicted by the best estimate design code CEFLASH-4AS. The trends and events of Table 5 which would be observed by the reactor operator are reproduced with similar timings. These include the intial abrupt pressurizer pressure and level drop, the pressure plateau, the departure of core exit fluid temperature from saturation to superheat conditions, the pressure stabilization, and the core exit fluid temperature peak followed by a decline. Comparison of the predicted primary pressures in Figure 17 shows good agreement in the details of the pressure history. The inner vessel level predicted by the simulator lags slightly behind that of the best estimate code, Figure 18, but shows the same overall behavior. The lag is due to simplifications in the simulator models. The good agreement is the result of the two-phase and nonequilibrium models which give the simulator the ability to realistically predict reactor behavior for severe accidents.

CONCLUSIONS

The C-E simulator thermal-hydraulic models are validated for a variety of events which must be represented by a simulator. The ability of the models to hold a steady state and handle symmetric and asymmetric single-phase pump transients is shown. The capability to predict measured PWR performance data for an overcooling transient involving nonequilibrium and two-phase conditions is demonstrated. The capacity of the models to reproduce the reactor behavior for severe transients, such as a small break LOCA, which is found with a best estimate design code is shown. The feasibility of developing and integrating models for the core, RCS and steam generator secondary systems which are based on design codes and which execute in real time is proven. The capability of the two-phase nonhomogeneous, nonequilibrium models is shown.

Use of models based on first-principle physics has extended the capability of the C-E simulator beyond that shown by earlier simulators. It can directly calculate a wide range of events—steady state, operational transients, and abnormal conditions such as total loss of feedwater, steam line break, steam generator tube rupture, anticipated transient without steam, and small and large break LOCAs. Full provision for operator intervention to change the course of the transient is available. Multiple failures and their interactions are permitted. The models are generic to a wide range of PWR plants with geometric model changes including noding accomplished through input data. Reality in the transient behavior is maintained to provide optimal operator training. Engineering calculations to support design studies and procedure development are possible.

ACKNOWLEDGEMENTS

The authors wish to acknowledge the significant technical contributions of H. L. Dolan and E. A. Forbes. Their effort in programming and debugging the models provided the calculational capability used for the analyses shown in the paper.

REFERENCES

1. Simulation Methods for Nuclear Power Systems, Proceedings of a Conference Held at Tucson, Arizona on January 26-28, 1981, EPRI WS-81-212, May 1981.

2. "Nuclear Power Plant Simulators for Use in Operator Training", ANS-3.5, November 20, 1980.

3. "Simulator Use and Development", Task I.A.4, "NRC Action Plan Developed as a Result of the TMI-2 Accident", NUREG-660, Volume 1, May 1980.

4. "CEFLASH-4AS, A Computer Program for the Reactor Blowdown Analysis of the Small Break Loss of Coolant Accident", CENPD-138, Supplement 1 (Non-proprietary), August 1974.

5. "Response of Combustion Engineering Nuclear Steam Supply System to Transients and Accidents", CEN-128, Vol. 1 (Non-proprietary), April 1980.

6. T. A. Porsching, et al., "FLASH-4: A Fully, Implicit FORTRAN IV Program for the Digital Simulation of Transients in a Reactor Plant", WAPD-TM-840, March 1969.

7. V. H. von Glahn, "An Empirical Relation for Predicting Void Fraction with Two-Phase Steam-Water Flow," NASA Technical Note D-1189, January 1962.

8. E. Isaacson and H. B. Keller, Analysis of Numerical Methods, John Wiley and Sons, Inc., New York (1966).

9. "Calculative Methods for the C-E Small Break LOCA Evaluation Model," CENPD-137, Supplement 1 (Non-proprietary), January 1977.

10. T. M. Anklam and M. D. White, "Experimental Investigations of Two-Phase Mixture Level Swell and Axial Void Fraction Distribution Under High Pressure, Low Heat Flux Conditions in Rod Bundle Geometry," pp. 4-67 to 4-88, ANS Specialists Meeting on Small Break Loss of Coolant Accident Analyses in LWRs, Monterey, California, EPRI WS-81-201, August 25-27, 1981.

11. S. G. Wagner and A. T. Shessler, "A Three Dimensional Improved Quasi-Static Core Model for Nuclear Reactor Control Room Simulators", to be presented at the Fifth Power Plant Dynamics, Control and Testing Symposium, Knoxville, Tennessee, March 21-23, 1983.

12. F. J. Moody, "Maximum Discharge Rate of Liquid-Vapor Mixtures from Vessels," ASME Winter Annual Meeting, November 1975.

13. "Combustion Engineering Analyses of LOFT Test L3-1", Combustion Engineering Submital to NRC, February, 1980.

14. S. Leichtberg and J. F. Kapinos, "C-E Analysis of LOFT Test L3-6", pp. 2-15 to 2-31, ANS Specialists Meeting on Small Break Loss of Coolant Accident Analyses in LWRs, Monterey, California, EPRI WS-81-201, August 25-27, 1981.

15. R. C. Mitchell, et al., "Verification of Best-Estimate Nuclear Power Plant Simulation Models", pp. 2-29 to 2-42, Simulation Methods for Nuclear Power Systems, EPRI WS-81-212, May, 1981.

FIGURE 1
PRIMARY SYSTEM GEOMETRIC MODEL

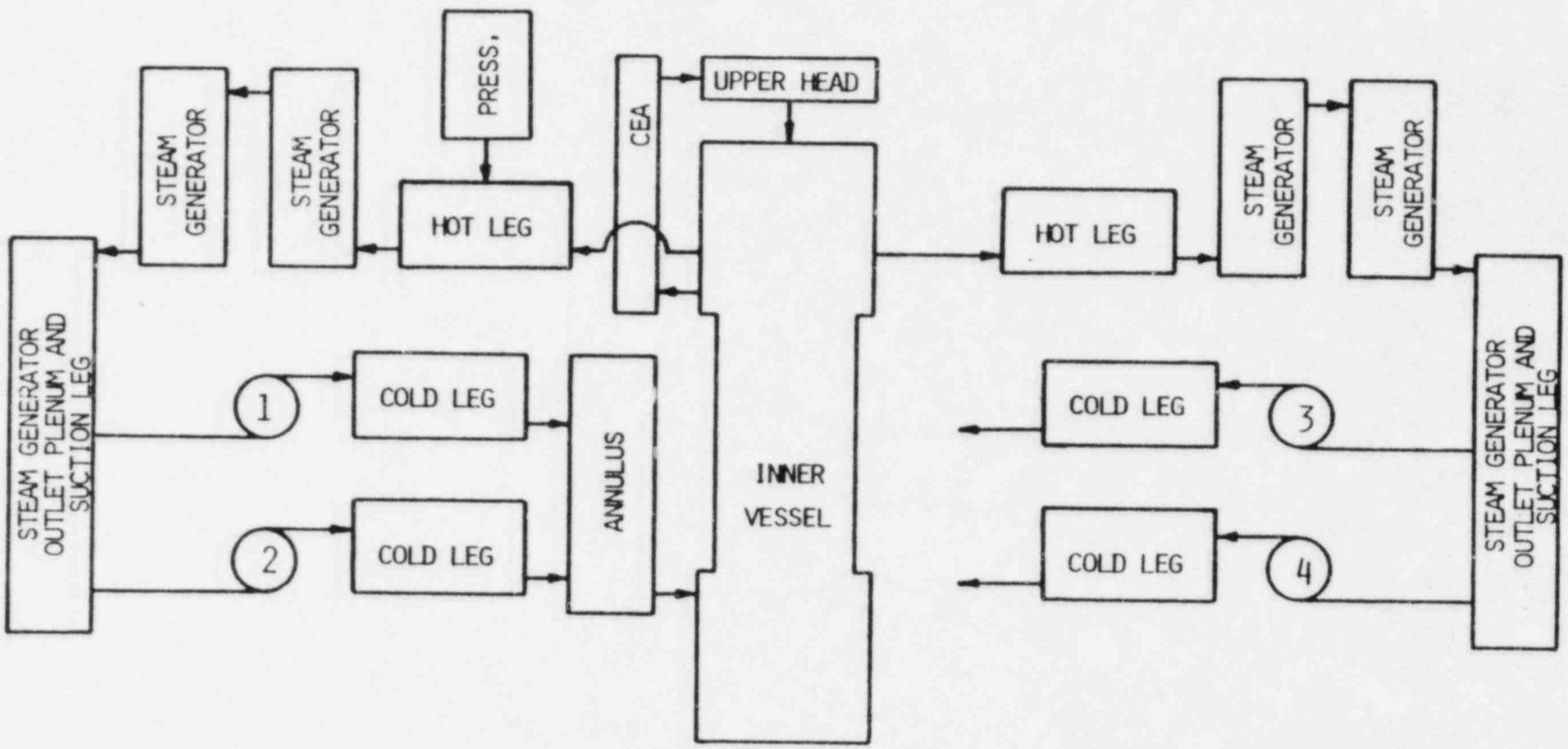

FIGURE 2
STEAM GENERATOR SECONDARY SYSTEM GEOMETRIC MODEL

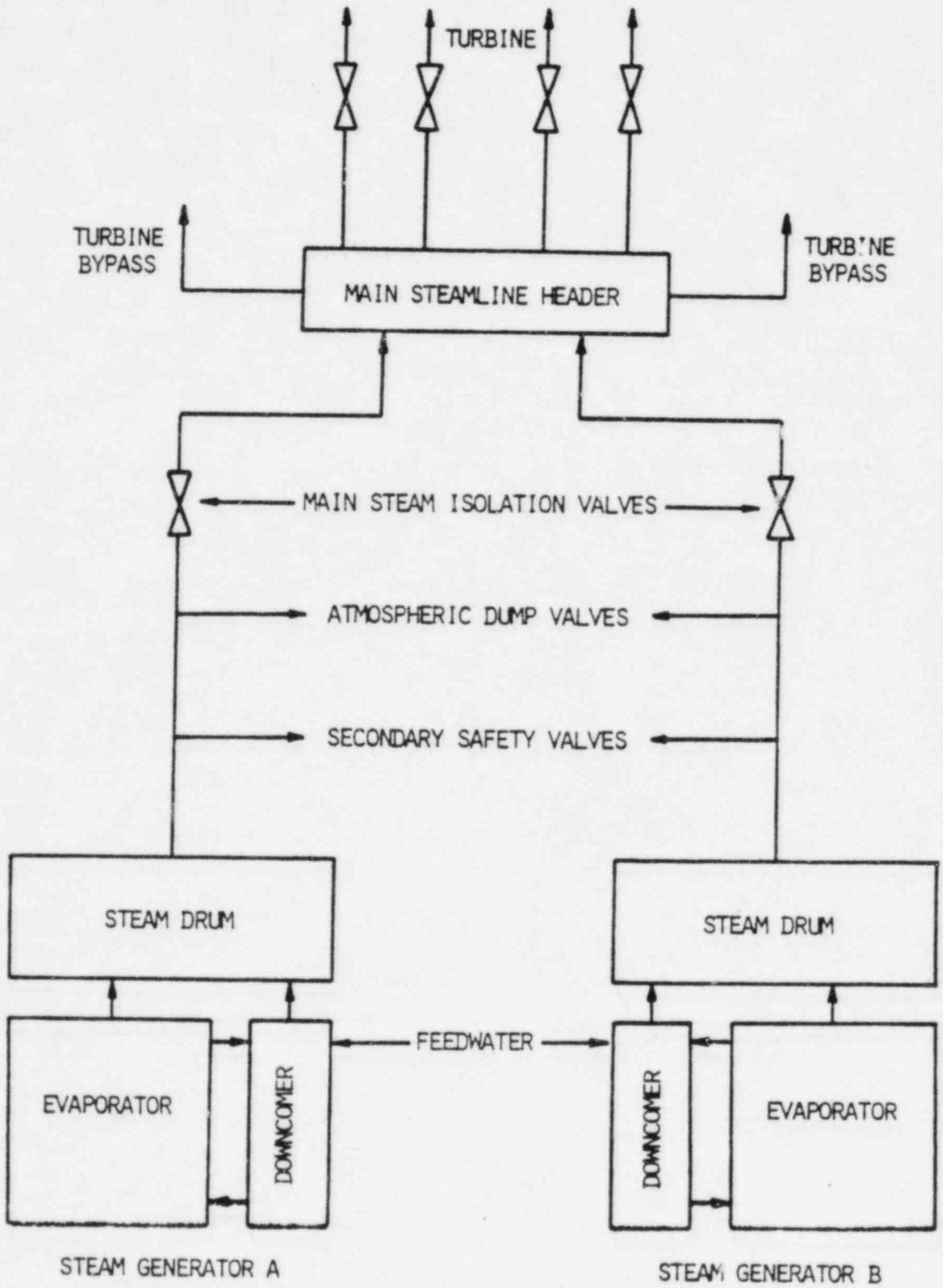

FIGURE 3
SMALL BREAK LOCA
(LOFT L3-1 TEST)

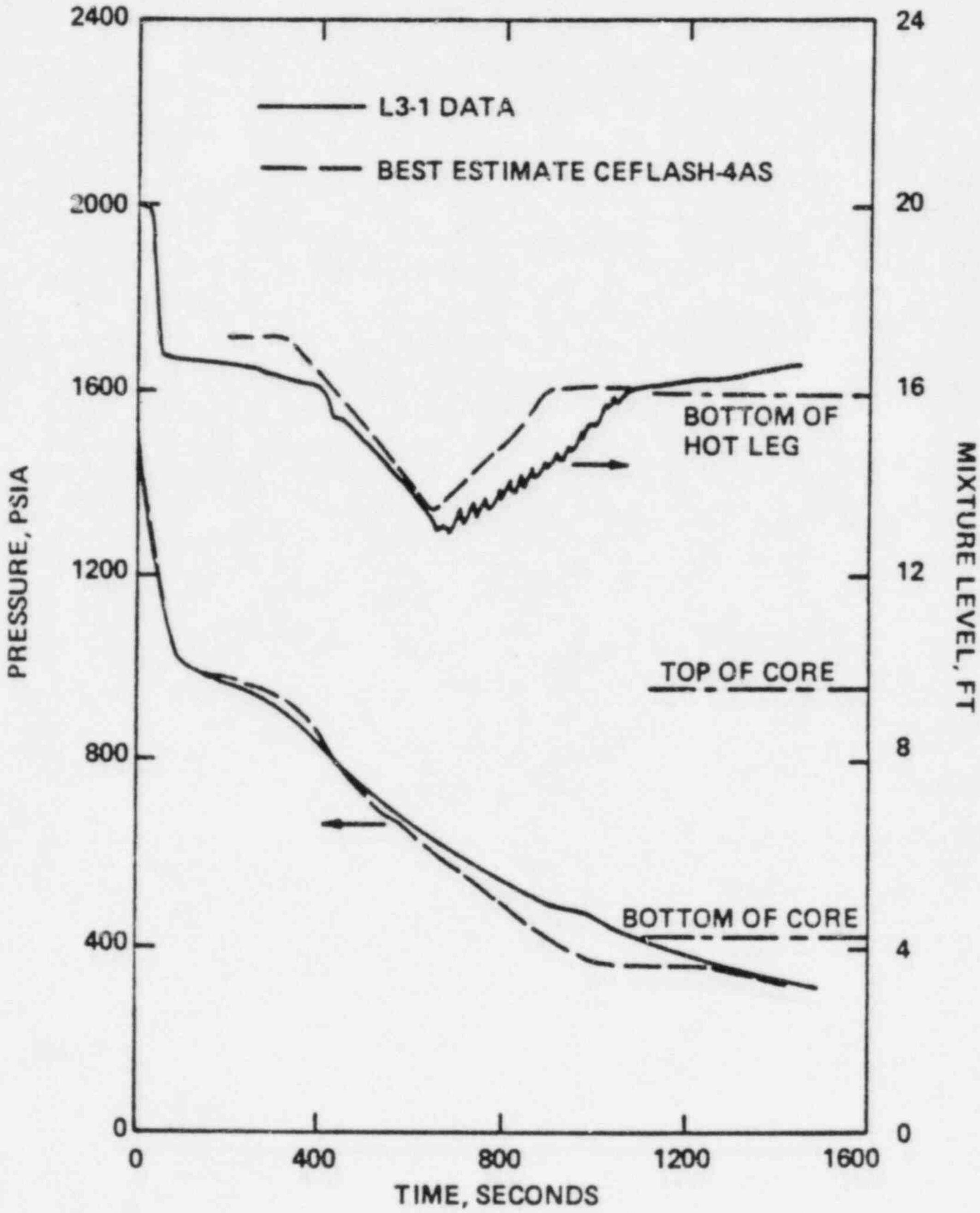

FIGURE 4

LOFT L3-6 PRIMARY SYSTEM PRESSURE

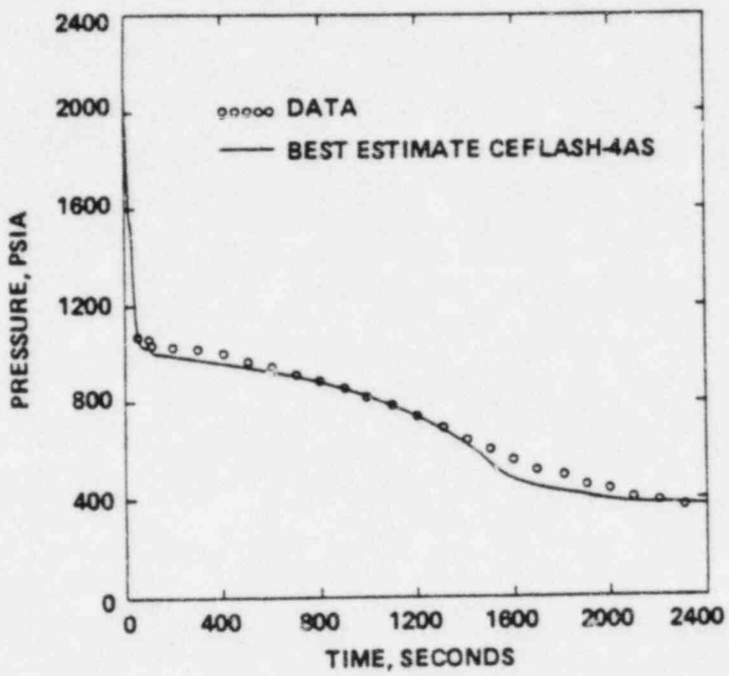

FIGURE 5

LOFT L3-6 PRIMARY SYSTEM MASS INVENTORY

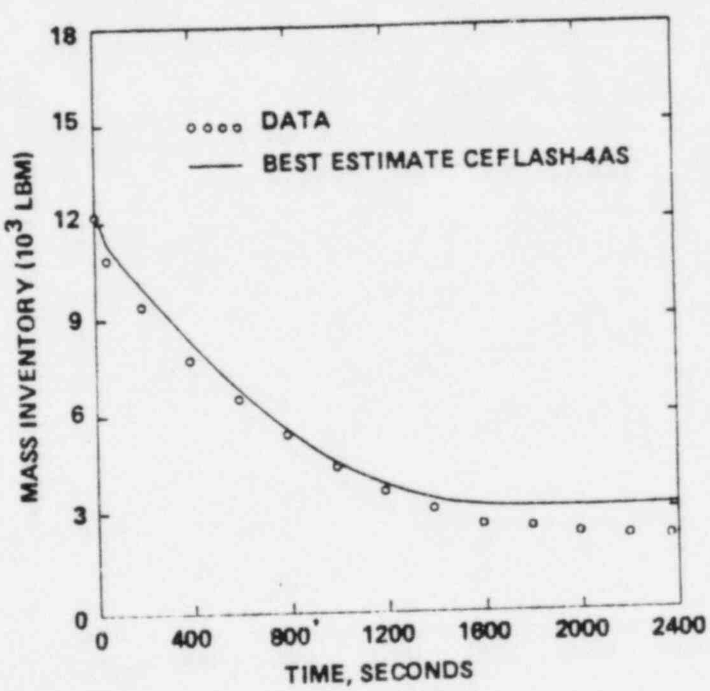

FIGURE 6
PRESSURIZER PRESSURE FOR PUMP TRANSIENT

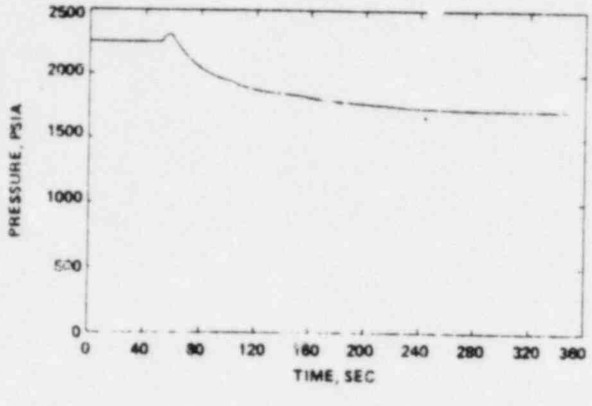

FIGURE 7
PRESSURIZER LEVEL FOR PUMP TRANSIENT

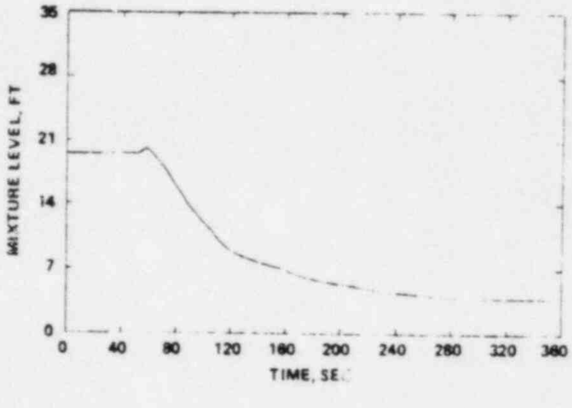

FIGURE 8
PUMP 1 FLOWRATE FOR PUMP TRANSIENT

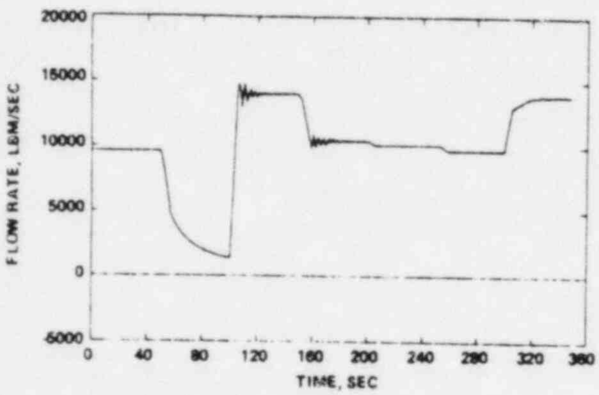

FIGURE 9
PUMP 2 FLOWRATE FOR PUMP TRANSIENT

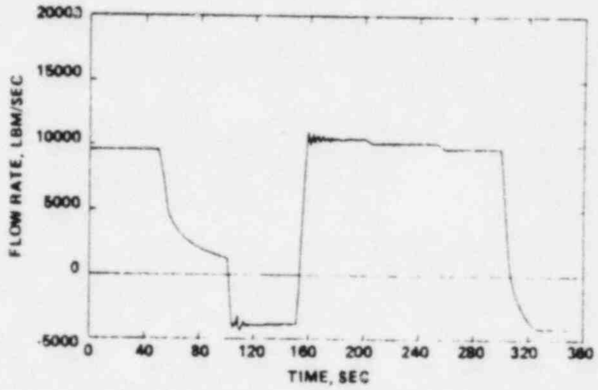

FIGURE 10
PUMP 3 FLOWRATE FOR PUMP TRANSIENT

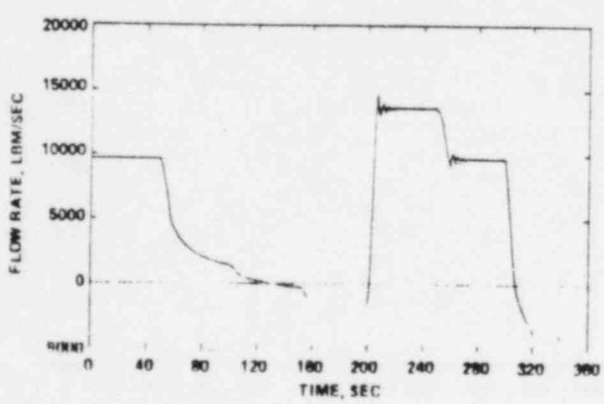

FIGURE 11
PUMP 4 FLOWRATE FOR PUMP TRANSIENT

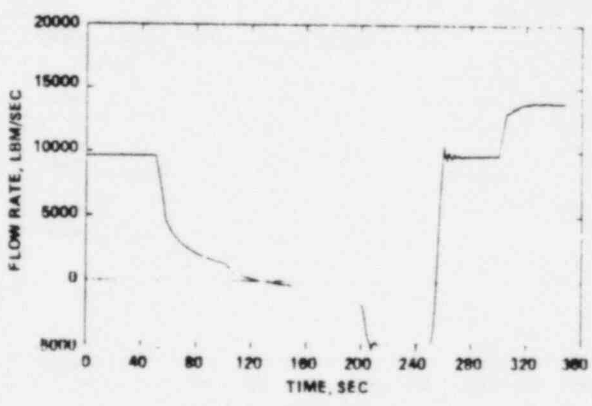

FIGURE 12
STEAM GENERATOR SECONDARY PRESSURE

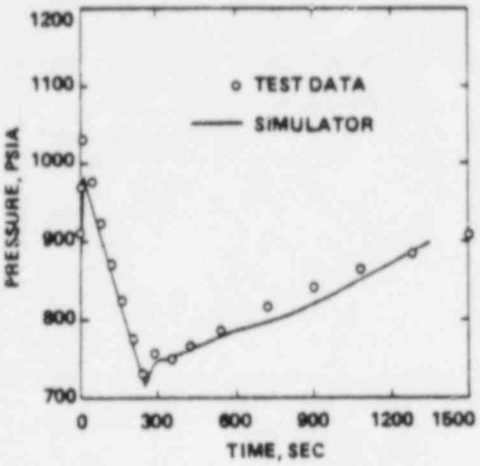

FIGURE 13
PRESSURIZER PRESSURE

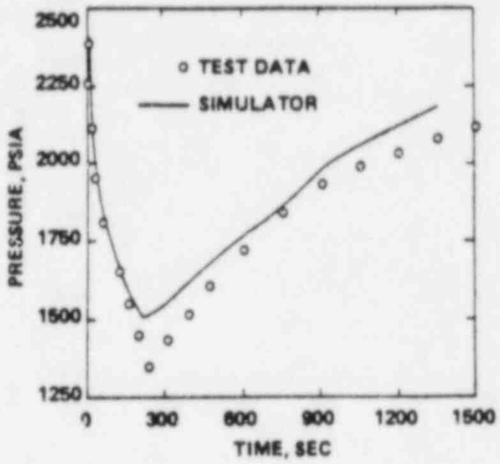

FIGURE 14
STEAM GENERATOR SECONDARY LEVEL

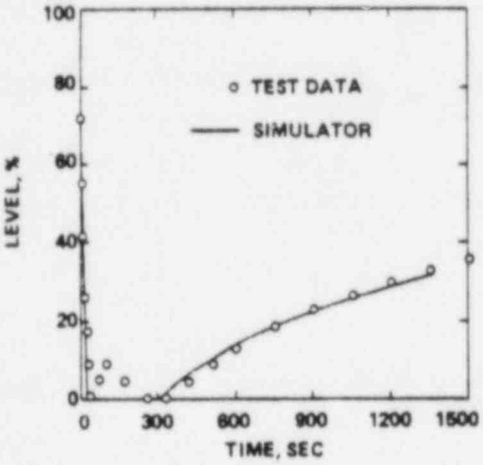

FIGURE 15
PRESSURIZER LEVEL

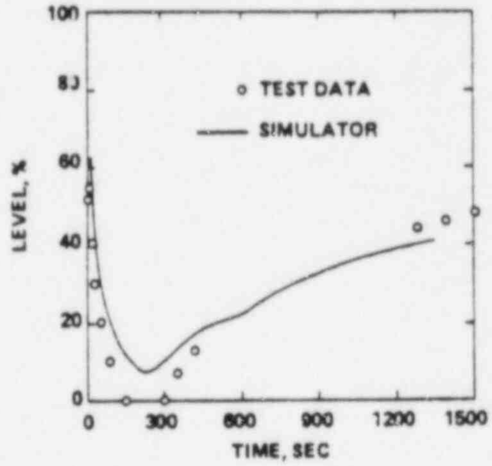

FIGURE 16
PRIMARY SYSTEM TEMPERATURES

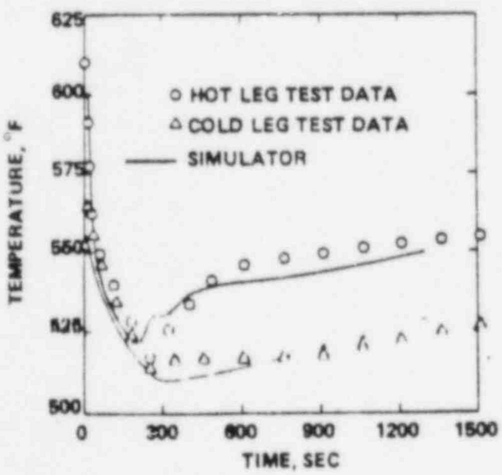

FIGURE 17
PRIMARY PRESSURE
FOR SMALL BREAK LOCA

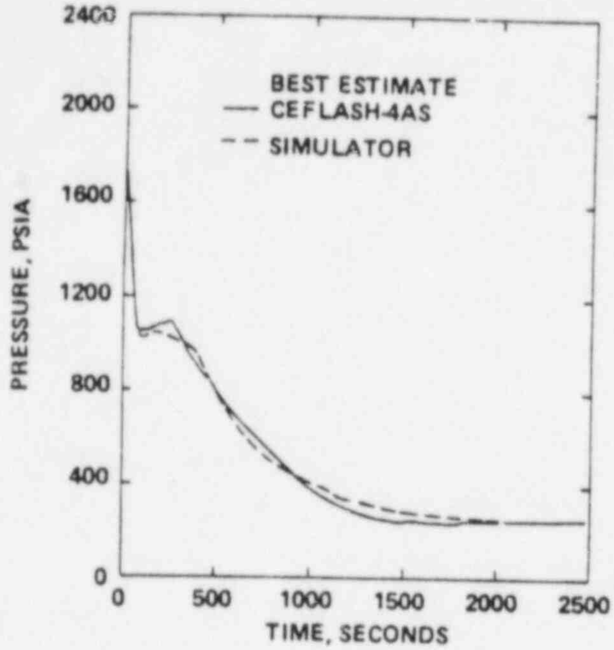

FIGURE 18
INNER VESSEL LEVEL
FOR SMALL BREAK LOCA

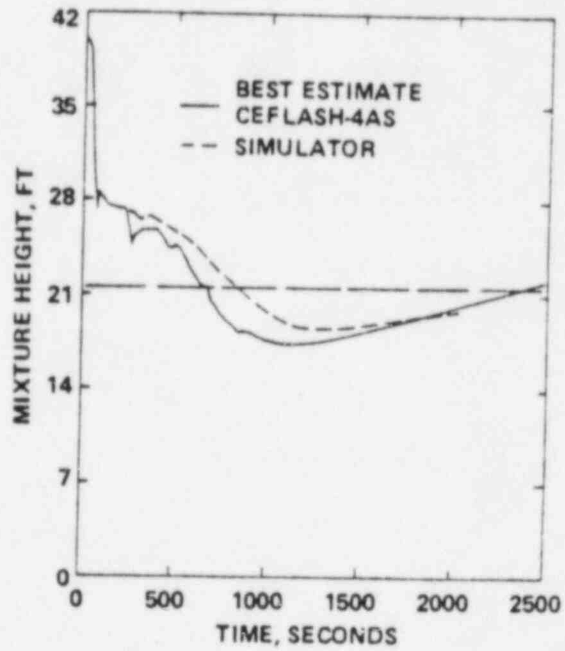

FIGURE 19
CORE EXIT STEAM TEMPERATURE
FOR SMALL BREAK LOCA

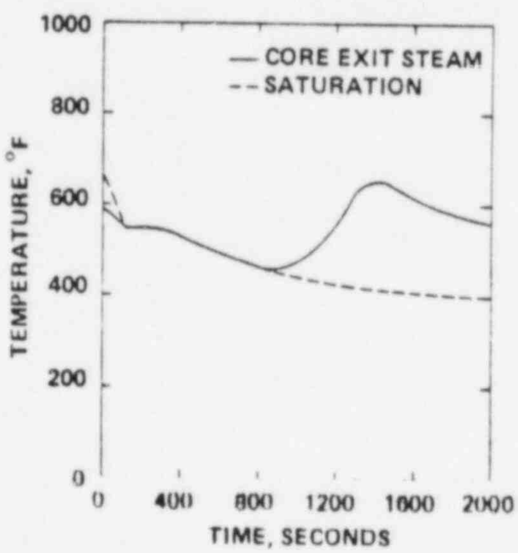

A THREE-DIMENSIONAL IMPROVED QUASI-STATIC CORE MODEL FOR NUCLEAR REACTOR CONTROL ROOM SIMULATORS

S. G. Wagner, A. T. Shesler

Nuclear Power Systems
Combustion Engineering, Inc.
Windsor, Connecticut

With the availability of powerful modern mini-computers, more sophisticated and accurate modeling is now expected of nuclear reactor control room simulators. Today, such simulators must model a wide range of operational and accident conditions which place great demands on computers and models. The core model in Combustion Engineering Calvert Cliffs I full scope control room simulator illustrates this trend. It features a full core, three-dimensional space-time neutronic and thermal-hydraulic model and runs on one of the simulator's Perkin Elmer 3244 computers using a small fraction of that machine's computing capability. The feasibility of using 3-D kinetics for real time simulation was demonstrated in Reference 1. Addition of thermal-hydraulics and a new approach to the improved quasi-static method (IQSM) are described here. The resulting model has successfully simulated operational and accident transients with a speed of 40 to 80 msec per reactor second. Thus, it fits easily into the real time requirements of the integrated simulator.

Structure of the Core Model

The goals of the model are to achieve realistic real time performance from an operator's viewpoint and demonstrate three-dimensional effects seen in the instrumentation and plant response. To do this, it is necessary to carry both core average and three-dimensional calculations for both neutronics and thermal-hydraulics. Core average calculations including point kinetics are performed several times per second to provide smooth and stable modeling of core dynamic conditions and to update the rapidly responding instruments. Three-dimensional calculations are performed every few seconds to take into account spatial effects of control rods, delayed neutrons and thermal-hydraulic asymmetries on instruments and primary system variables. In addition, a single core average fuel pin and flow channel with greater axial and radial detail is modeled with a one second time step to determine heat transfer conditions over a wide variety of core heat transfer situations. This structure is illustrated in Figure 1.

In the 3-D neutronics model, each assembly is divided into 4 axial nodes for a total of 868 nodes. While there are probably more nodes than the minimum needed to demonstrate the spatial effects seen by the operators, the large number of nodes permits several simplifications in modeling control rods and instruments. For example, there is never more than one control rod inserted in a node. Complex questions of nodal cross section and coupling changes under various combinations of normal and abnormal rod insertion are avoided. Rod shadowing effects on instruments are calculated automatically. Meanwhile, the xenon, decay heat, and thermal-hydraulic models require only 132 nodes. Other simplifications further reduce the computational and memory requirements of an 868 node core model. Hence, the model has proven to be simpler to supply with data than a model with fewer nodes, yet it is still fast running and efficient in its use of memory.

Neutronics Model

The neutronics model is a new form of the improved quasi-static method (IQSM)[2] applied to a one-group FLARE-like 3-D nodal model[3]. In the IQSM, the space and time-dependent power distribution P is factored into a time-dependent amplitude T and a normalized time-dependent shape S. The power in one of the 868 nodes L is expressed

$$P_L(t) = T(t)\, S_L\,(t) \tag{1}$$

where

$$\sum_L S_L\,(t) = ||S|| = \text{constant.} \tag{2}$$

The differential equations for P_L and its associated six-group delayed neutron source are

$$\Lambda \frac{\partial P_L}{\partial t} = (1-\beta) k_{\infty L} \sum_M W_{ML} P_M - P_L + \sum_n C_{nL} + S_L^B \tag{3}$$

$$\frac{\partial C_{nL}}{\partial t} = \lambda_n \left(\beta_n\, k_{\infty L} \sum_M W_{ML}\, P_M - C_{nL}\right) \tag{4}$$

where

Λ = prompt neutron lifetime

$k_{\infty L}$ = node L infinite multiplication factor

W_{ML} = probability that a neutron born in node M will be absorbed in node L

C_{nL} = delayed neutron source from precursor group n in node L

S_L^B = background source including photoneutrons

β, β_n = total and group n delayed neutron fraction

and where power and fission rate are assumed to be proportional. From these equations, point kinetics equations for T and C_n (the core average delayed neutron sources) are derived:

$$\frac{\Lambda}{k_{eff}} \frac{\partial T}{\partial t} = (\rho - \beta) T + \frac{\sum_n C_n + \sum_L S_L^B}{k_{eff}} \tag{5}$$

$$\frac{\partial C_n}{\partial t} = \lambda_n (\beta_n k_{eff} T - C_n) \tag{6}$$

where we define

$$k_{eff}(t) = \frac{\sum_L k_{\infty L}(t) \sum_m W_{ML} S_M}{||S||} \tag{7}$$

and

$$\rho(t) = 1 - 1/k_{eff}(t). \tag{8}$$

These are integrated implicitly over small timesteps from t to $t+\delta t$ using an exponential approximation for the prompt neutrons and backwards differencing for the delayed neutrons:

$$T(t+\delta t) = T(t)e^{\omega\delta t} + (1 - e^{\omega\delta t}) \frac{\sum_n C_n(t) + \sum_L S_L^B(t)}{[\beta - \rho(t+\delta t)]\, k_{eff}(t+\delta t)} \tag{9}$$

$$C_n(t+\delta t) = \frac{C_n(t) + \lambda_n \beta_n T(t+\delta t)\,\delta t}{1 + \lambda_n \delta t} \tag{10}$$

where we have defined a prompt frequency, ω, to be

$$\omega = \frac{[\rho(t+\delta t) - \beta]\, k_{eff}(t+\delta t)}{\Lambda}. \tag{11}$$

When the core is very near to prompt critical, ω approaches zero and equation 9 degenerates to the following limiting form. This must be used to prevent equation 9 from becoming indefinite:

$$T(t+\delta t) = T(t) + \frac{\delta t}{\Lambda} [\sum_n C_n(t) + S^B(t+\delta t)]. \tag{12}$$

In most sub-prompt critical cases, the exponentials in equation 9 are small enough to be taken as zero. In these cases equation 9 is equivalent to the prompt jump approximation. An automatic time step selection procedure is used to prevent power from increasing too far before the effects of Doppler feedback are included. This is important in prompt critical situations.

If we assume the last 3-D calculation was performed at time $t^* < t$, it is necessary for point kinetics to estimate k_{eff} using the latest available rod positions and core average thermal-hydraulic conditions. This is done as follows:

$$k_{eff}(t) = k_{eff}(t^*) + \sum_L \Delta k_{\infty L}^{rods} \left(\sum_M W_{ML}\ S_M(t^*)/\ ||S||\right) + \left(\sum_i \frac{\partial \bar{k}}{\partial X_i} \Delta X_i\right)\left(\sum_L \sum_M W_{ML}\ S_M(t^*)/\ ||S||\right) \tag{13}$$

where ΔX_i are changes in various core average thermal-hydraulic parameters and $\Delta k_{\infty L}^{RODS}$ is the local change in k_∞ due to rod motion since t^*. This calculation can be performed very quickly because rods move in a relatively few nodes and because two of the sums can be precalculated. Any errors in this approximation will be corrected when the next 3-D calculation is completed.

After several seconds, a new 3-D shape calculation is initiated. This calculation is based on conditions in the core at time $t'>t^*$. Due to the number of operations and the need to allow time for other models to be updated, the 3-D calculation is divided into segments and run over several point kinetics timesteps. It is completed at time t'', several point kinetics steps later. This timing is illustrated in Figure 2.

A single delayed neutron group is carried in 3-D by making the approximation that the six groups are in the same proportion everywhere. Implicit equation for the 3-D shape and delayed neutron source C_L can be derived. The shape equation is

$$S_L(t')\left[\frac{\cdot}{t'-t^*} + \frac{\Lambda}{\delta t}\ \frac{T(t')-T(t'-\delta t)}{T(t')}\right] - \frac{S_L(t^*)\Lambda}{t'-t^*}$$

$$= (1-\beta+f_2/T(t'))\ k_{\infty L} \sum_M W_{ML}\ S_M(t') - S_L(t') + \frac{f_1\ C_L\ (t^*)}{T(t')} + \frac{S_L^B}{T(t')} \tag{14}$$

where from the point kinetics

$$f_1 = \sum_n C_n\ (t^*)e^{-\lambda_n(t'-t^*)}/\ \sum_n C_n(t^*) \tag{15}$$

and

$$f_2 = \frac{\Sigma C_n(t') - C_n(t^*)e^{-\lambda_n(t'-t^*)}}{k_{eff}(t')\ T\ (t')} \tag{16}$$

In computing the above two factors, the following approximation must be used to be consistent with the differencing method in equation 10:

$$e^{-\lambda_n(t'-t^*)} = \prod_i \frac{1}{1+\lambda_n \delta t_i} \tag{17}$$

where the δt_i represent the point kinetics time steps in the interval t^* to t'.

A limited number of iterations of equation 14 are performed each 3-D time step. When necessary to improve stability, the 3-D thermal-hydraulic calculation may be iterated with the neutronics. When the iterations are done, the 3-D delayed neutron source is updated:

$$C_L(t') = f_1\, C_L(t^*) + f_2\, T(t')\, k_{\infty L} \sum_M W_{ML}\, S_L(t'). \tag{18}$$

When the 3-D calculation is completed at time t", the reactivity calculated from 3-D may differ from the estimated point kinetics reactivity and the shape may no longer be normalized. We adjust k_{eff} as follows:

$$k_{eff}^{POINT\ KIN}(t") \leftarrow k_{eff}^{POINT\ KIN}(t") + k_{eff}^{3-D}(t') - k_{eff}^{POINT\ KIN}(t') \tag{19}$$

Then, if we find

$$\alpha = \frac{||S_L||}{\sum_L S_L(t')} \neq 1, \tag{20}$$

where the numerator represents the desired normalization, we perform the following renormalizations of both 3-D and point kinetics:

$$T(t") \leftarrow T(t")/\alpha \tag{21}$$

$$S_L(t') \leftarrow \alpha S_L(t') \tag{22}$$

$$C_n(t") \leftarrow C_n(t^*)e^{-\lambda_n(t"-t^*)} + \frac{k_{eff}^{3-D}(t')}{\alpha k_{eff}^{POINT\ KIN}(t')} \left[C_n(t') - C_n(t^*)e^{-\lambda_n(t"-t')}\right]. \tag{23}$$

Equation 23 can be viewed as the sum of a simply decaying term due to precursors present at time t* and an adjusted term due to precursors created after t*. The 3-D delayed neutron source C_L does not require adjustment since the adjustments to T and S would cancel in equation 18.

Fuel Temperature Model

Three parallel fuel temperature calculations are carried. These are 1) a core average calculation carried with the point kinetics, 2) a 12-region axial calculation carried as part of the detailed heat transfer, and 3) a 3-D calculation with 33 nodes in each of 4 axial levels for use in the 3-D neutronics calculations. All three models are lumped parameter models of the following form:

$$\begin{bmatrix} C^{FUEL} \dfrac{\partial T^{FUEL}}{\partial t} \\ C^{CLAD} \dfrac{\partial T^{CLAD}}{\partial t} \end{bmatrix} = \begin{bmatrix} -h^{FC} & h^{FC} \\ h^{FC} & (-h^{FC} - h^{CM}) \end{bmatrix} \begin{bmatrix} T^{FUEL} \\ T^{CLAD} \end{bmatrix} + \begin{bmatrix} P^{SENS} \\ h^{CM}\, T^{MOD} \end{bmatrix} \tag{24}$$

where

C^{FUEL}, C^{CLAD} = fuel and clad heat capacities

h^{FC}, h^{CM} = effective fuel-clad and clad-moderator heat transfer coefficients

T^{FUEL}, T^{CLAD}, T^{MOD} = fuel, clad, moderator temperatures

P^{SENS} = sensible power appearing in the node (includes decay heat)

The 12-region axial calcualtion carries the most detail in determining C^{FUEL}, C^{CLAD}, h^{FC} and h^{CM}. It is capable of representing a wide range of subcooled, boiling and steam core heat transfer conditions. This model is used to provide constants for the core average and 3-D models. In the 3-D model, separate constants are computed for each of its four axial levels.

Decay heat for the core average model is computed using eleven groups. Effective decay constants for 3 larger groups are computed from this model and these three groups are used in the 3-D model. Axial shapes for the prompt and decay heat release are computed in the 3-D model and these are synthesized and smoothed using data from the core average model to provide a 12-node axial power distribution for the detailed heat transfer calculation.

Coolant Model

As with the fuel temperature model there are also three calculations of coolant conditions in the core. For use in point kinetics, the core average moderator conditions are taken from a node of the reactor coolant system model. A sophisticated bubble rise model taken from CEFLASH-4A[4] and PARCH[5] is used for the 12 node detailed axial heat transfer model. Finally, for feedback to the 3-D neutronics, a model with 33 closed channels, four nodes high is used. To simulate crossflow mixing under low flow conditions,the code assumes no crossflow mixing at full flow varying gradually to complete mixing at low or reverse flow (i.e. uniform radial enthalpy). By this approach important 3-D reactivity effects seen in steamline break[6] and other transients can be approximated without the added computations required for a true 3-D crossflow model. Details about reactor coolant system and ohter process models in the simulator are given in Reference 7.

The following equation shows how the outlet enthalpy h^{OUT} for one of the 3-D nodes is calculated

$$h^{OUT}(t') = (1-f^{B}) \frac{h^{OUT}(t^{*}) + R(t')\, h^{IN}(t') + (t'-t^{*}) v\, Q}{1 + R(t')} + f^{B}\, h^{OUT}_{AVG}(t') \qquad (25)$$

where

h^{IN}, h^{OUT}	= node inlet, outlet enthalpy
h^{OUT}	= average outlet enthalpy for nodes at this level when taken from the 12-node detailed heat transfer model.
f^B	= mixing factor; $0 \leqslant f^B \leqslant 1.0$
R	= nodes traversed by coolant in one time step (t'-t*)
Q	= local heat source in the coolant
v	= coolant specific volume

It should be noted that f^B is a function of the static head across the core and the total pressure drop across the core. Under reverse flow conditions where equation 25 would be unstable, f^B is one and the first term is not calculated. The detailed heat transfer calculation uses a flow model which is stable under all flow conditions. Use of a radially uniform enthalpy distribution is physically reasonable under many such conditions and any errors introduced in 3-D core calculation would not be important to the operator under these conditions.

Instrument Signals

The core model computes three kinds of signals: ex-core neutron detectors, in-core neutron detectors and core exit thermocouples. Ex-core signals are a weighted sum of nearby node powers and are corrected for density changes in the water surrounding the core. The ex-core signals automatically reflect rod movement because the current 3-D power distribution is used. In-core detector signals are taken directly from the 3-D power distribution and are again temperature compensated. Thermocouple readings are computed using core outlet conditions from the 3-D coolant model. They are corrected for bypass flow through the instrument guide tubes and the possibility of reverse flow is taken into account.

Test Results

Several test results have been selected to illustrate the salient features of the model. For all the results shown, the core model was isolated from other simulator models. Parameters such as rod position, inlet conditions and pressure which are normally computed by other models were input by hand.

Figure 3 shows the core model response to conditions similar to those after a loss of feedwater. In order to force the calculation into saturated conditions, no scram was simulated. The inlet enthalpy, which was input by hand, is also plotted. Because saturated conditions exist in the core during much of the transient, a good test of the major components of the core model is provided. Shown on the power plot is a comparable calculation by the C-E design codes. Other tests not shown have brought the core model to saturation while critical with various moderator coefficients. No anomalous behavior such as feedback oscillations between 3-D neutronic and thermal-hydraulics has been observed.

Figures 4 and 5 show core power after a scram from hot full power. The rods were inserted over a three second interval. On Figure 4 the effect of the 3-D calculation is barely perceptible. To illustrate the timing of the 3-D calculation once again and to quantify the effect of the renormalization, Figure 5 shows a portion of the transient with expanded scale. The jump in power due to renormalization is not observable by the trainees on the normal power level instrumentations. However, some care must be taken in providing signals for the startup rate ($\partial \log_{10} P/\partial t$) meters. The effect of the renormalization on this signal is spread out over the time between 3-D calculations and the meters perform smoothly.

Two transients which demonstrate the desirability of having a 3-D nodal model have been included. The first is an asymmetric rod drop at hot full power. Figures 6 and 7, respectively, show the power shape in one horizontal plane before and after the rod drop. The position of the dropped rod is indicated on Figure 7. On Figure 8 two ex-core instrument signals and core power are plotted versus time. The immediate reduction in core power is seen. Then as shape changes and feedbacks bring total core power back up somewhat, the two signals separate. (Because the core model is being run with a constant inlet temperature in this test, the power does not return to 100% as it does with the fully integrated model). The effect of distributed delayed neutrons on power shape can be seen in the gradual approach of the instrument signals to their asymptotic signals. The sharp change in slope and the fact that the three curves do not separate for the first few seconds are numerical effects caused by the use of point kinetics between 3-D calculations.

Spatial effects can also be seen under asymmetric thermal-hydraulic conditions. Figure 9 shows a power distribution with a 20°F temperature difference across the inlet. Such a condition could arise in certain secondary system transients or in part loop operation. The 3-D nodal model calculates the power distribution and its impact on all instrument signals. It also provides a difference in outlet temperature to the two hot legs of the reactor coolant system.

At this point, a word about running time is appropriate. Under steady state conditions one 3-D iteration per 3-D time step is sufficient and the model runs in .040 central processor seconds per simulated second. Under transient conditions involving rod motion or significant thermal-hydraulic changes more 3-D iterations may be required. Up to .080 central processor seconds per simulated second are required. These running times are averaged over thirty seconds.

Conclusion

The nodal 3-D core simulator model using a variant of the improved quasi-static method has successfully modeled transient conditions encountered in operator training. The trainee is provided an opportunity to observe, understand and diagnose abnormal core conditions for a wide variety of events which frequently involve spatial effects. The 40 to 80 msec/ sec speed of the model makes it fit easily within the real time simulation requirements of the integrated simulator.

References:

1. J. W. Earles, S. G. Wagner, R. G. Foster, "FRST-A Fast Running Space Time Kinetics Code for Use in Nuclear Power Plant Simulation", Summer Computer Simulation Conference, July 19-21, 1982, Denver, Colorado.

2. "FIESTA: A One-Dimensional, 2-Group Space Time Kinetics Code for Calculating PWR SCRAM Reactivities", CEN-133 (B), November, 1979.

3. D. L. Fisher, J. M. Harriman, M. J. Stedwell, "FLARE, A Three Dimensional Boiling Water Reactor Simulator", GEAP 4598, July, 1964.

4. "CEFLASH-4A: A FORTRAN-4 Digital Computer Program for Reactor Blowdown Analysis", CENPD-133, August 1974.

5. "PARCH: A FORTRAN 4 Digital Program to Evaluate Pool Boiling Axial Rod and Coolant Heating", CENPD-138, August, 1974.

6. S. G. Wagner et al., "Thermal-Hydraulic Models for Use in Simplified Reactivity Calculations Under Secondary Break Conditions," Proc. Int. Topical Mtg. Advances in Mathematical Methods for the Solution of Nuclear Engineering Problems, April 27-29, 1981, p. 613.

7. R. J. Espinosa, R. L. McBeth, P. K. Doherty, "Application of Thermal Hydraulics Design Codes to Real Time PWR Simulation", to be published Fifth Power Plant Dynamics Control and Testing Symposium, Knoxville, Tennessee, March 21-23, 1983.

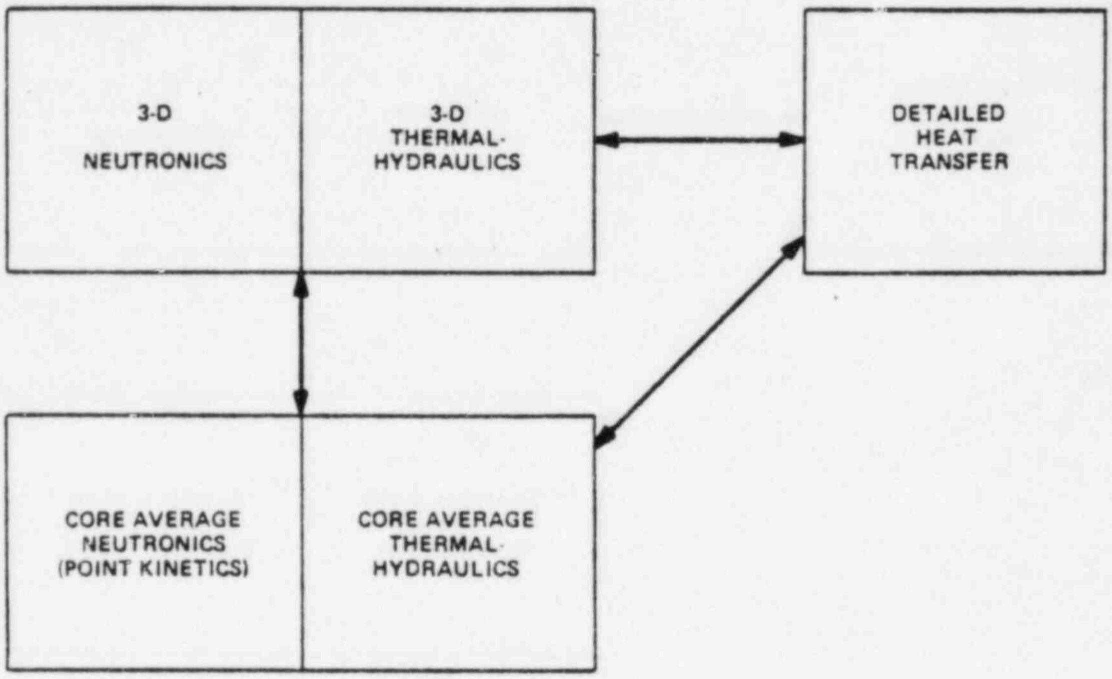

FIGURE 1: STRUCTURE OF THE CORE MODEL

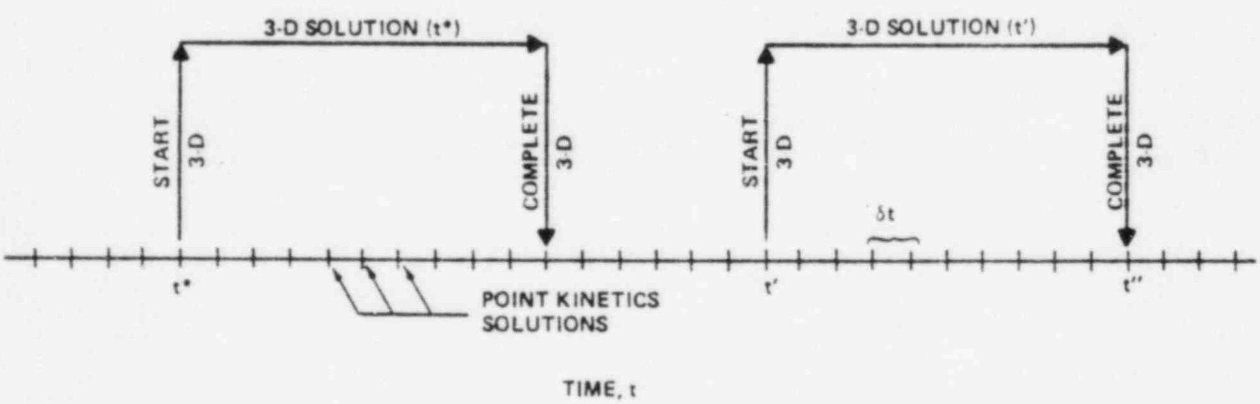

FIGURE 2: TIMING OF CORE NEUTRONICS CALCULATIONS

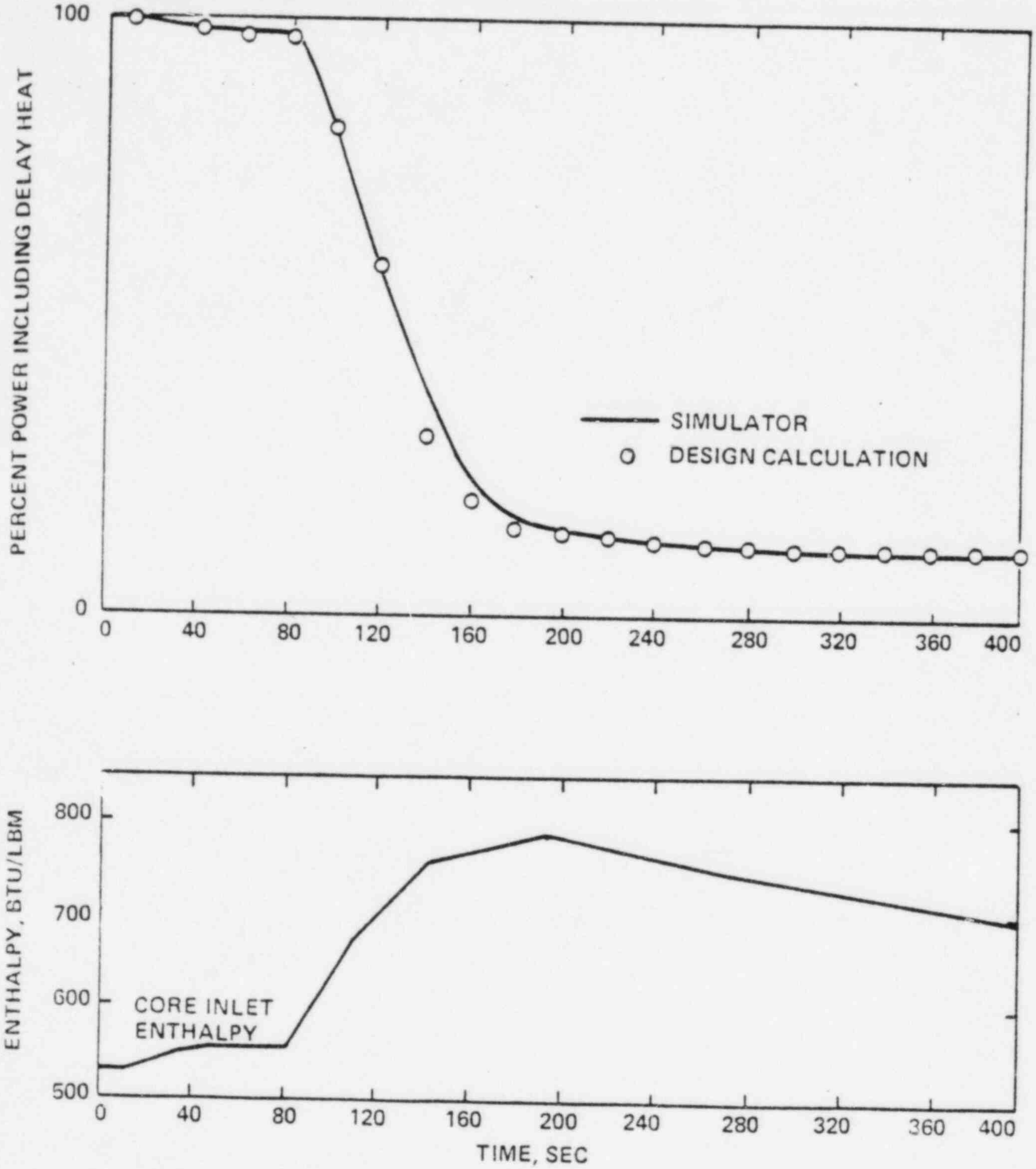

FIGURE 3: RESPONSE TO COMPLETE LOSS OF FEEDWATER

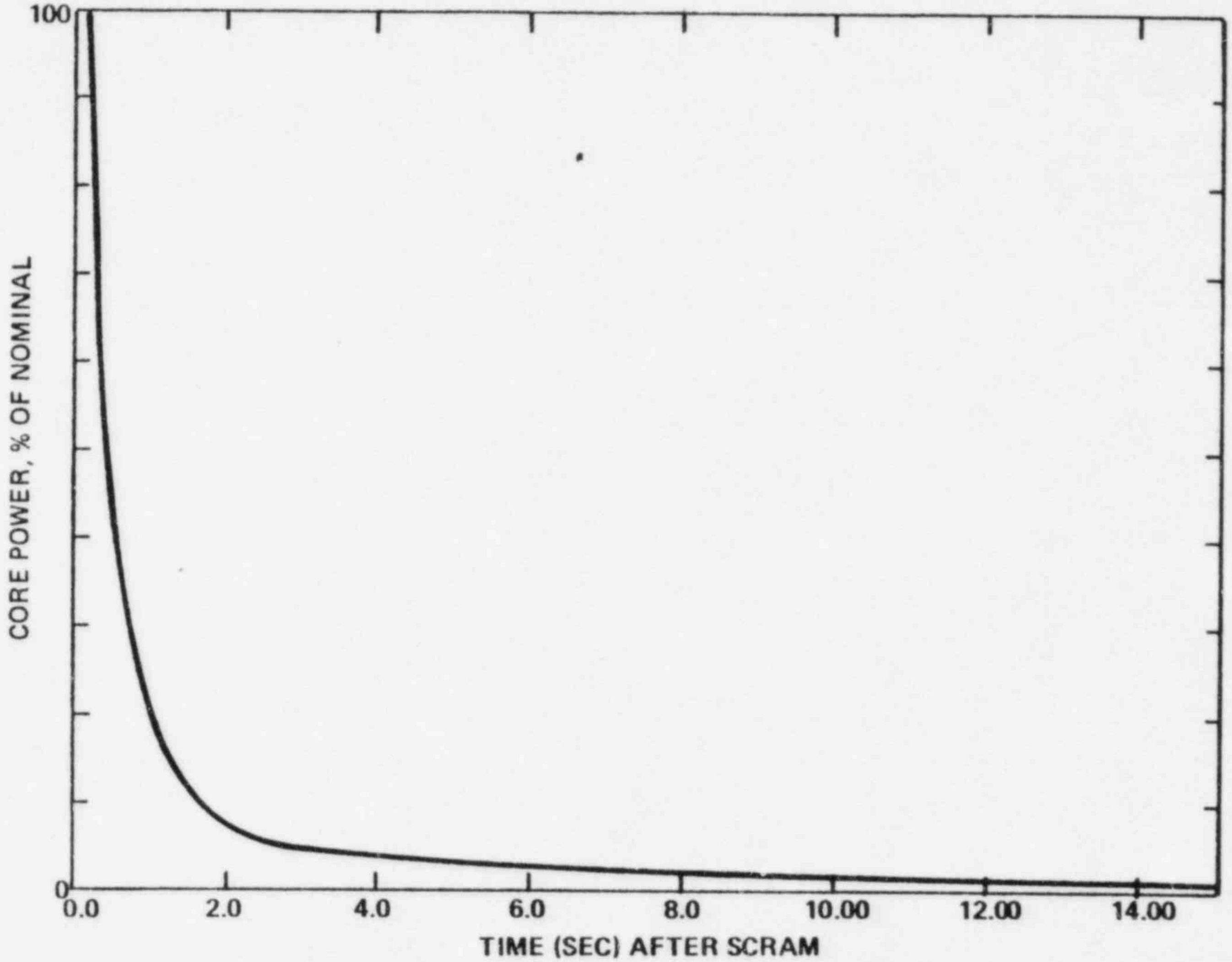

FIGURE 4: CORE POWER AFTER A SCRAM FROM FULL POWER

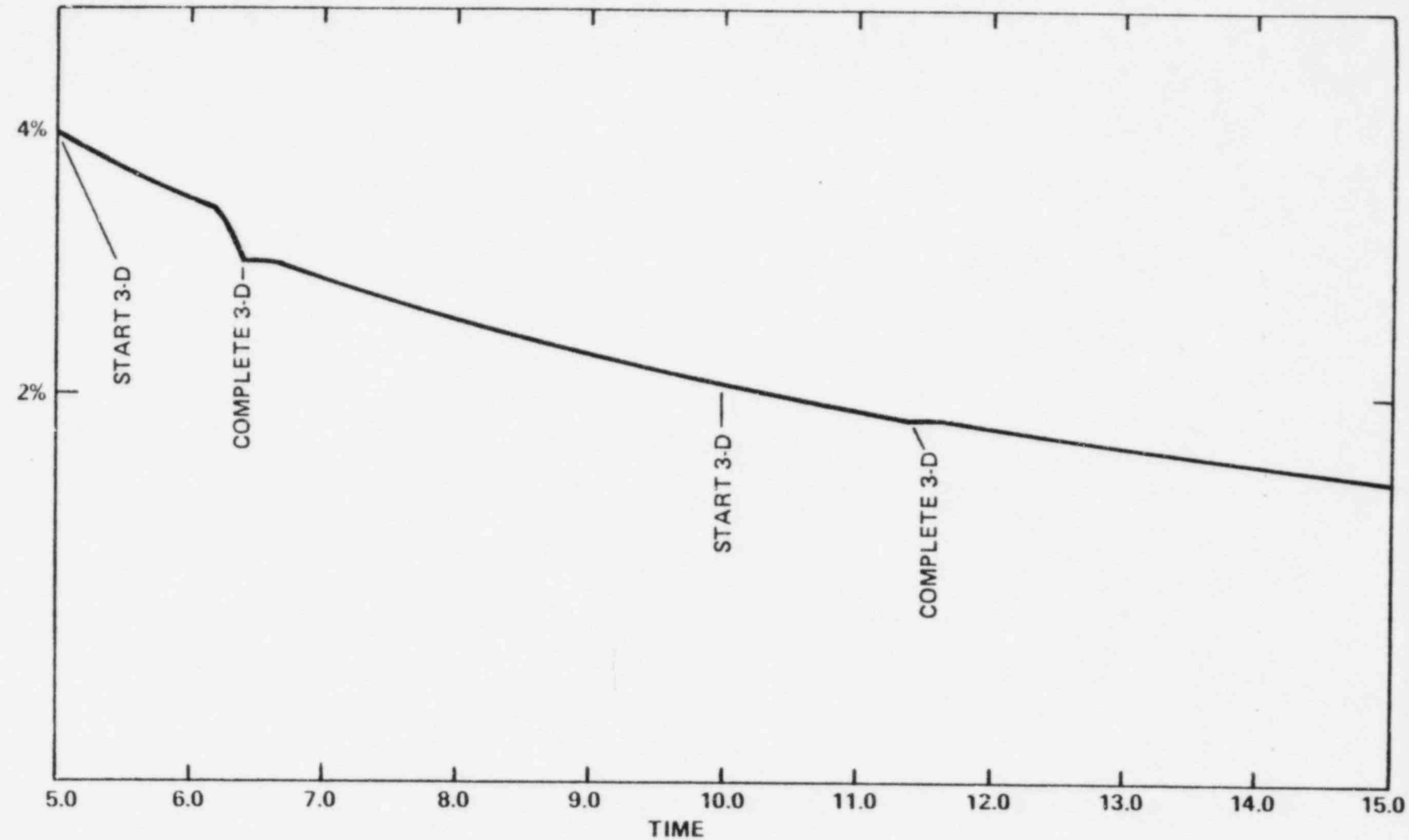

FIGURE 5: CORE POWER VERSUS TIME ON EXPANDED SCALE TO SHOW EFFECT OF 3-D RENORMALIZATION AFTER SCRAM

							0.85	1.14	1.14	0.85						
				0.86	1.15	1.15	1.14	1.13	1.14	1.15	1.15	0.86				
			0.97	1.27	1.16	1.39	1.07	1.43	1.07	1.39	1.16	1.27	0.97			
		0.97	1.23	1.19	1.44	1.12	1.37	1.39	1.37	1.12	1.44	1.19	1.23	0.97		
	0.86	1.27	1.22	1.38	1.13	1.36	1.18	1.35	1.18	1.36	1.13	1.38	1.22	1.27	0.86	
	1.15	1.15	1.44	1.13	1.43	1.14	1.40	1.01	1.40	1.14	1.43	1.13	1.44	1.15	1.15	
	1.15	1.39	1.12	1.36	1.14	1.27	1.10	1.21	1.10	1.27	1.14	1.36	1.12	1.39	1.15	
0.85	1.14	1.07	1.38	1.18	1.40	1.10	1.33	1.07	1.33	1.10	1.40	1.18	1.38	1.07	1.14	0.85
1.13	1.12	1.44	1.41	1.34	1.00	1.19	1.09	0.80	1.09	1.19	1.00	1.34	1.41	1.44	1.12	1.13
1.13	1.14	1.07	1.38	1.18	1.40	1.10	1.33	1.07	1.33	1.10	1.40	1.18	1.38	1.07	1.14	1.13
0.85	1.15	1.39	1.12	1.36	1.14	1.27	1.10	1.21	1.10	1.27	1.14	1.36	1.12	1.39	1.15	0.85
	1.15	1.15	1.44	1.13	1.43	1.14	1.40	1.01	1.40	1.14	1.43	1.13	1.44	1.15	1.15	
	0.86	1.27	1.22	1.38	1.13	1.36	1.18	1.35	1.18	1.36	1.13	1.38	1.22	1.27	0.86	
		0.97	1.23	1.19	1.44	1.12	1.37	1.39	1.37	1.12	1.44	1.19	1.23	0.97		
			0.97	1.27	1.16	1.39	1.07	1.43	1.07	1.39	1.16	1.27	0.97			
				0.86	1.15	1.15	1.14	1.13	1.14	1.15	1.15	0.86				
							0.85	1.14	1.14	0.85						

FIGURE 6: POWER SHAPE AT FULL POWER FOR ONE HORIZONTAL PLANE

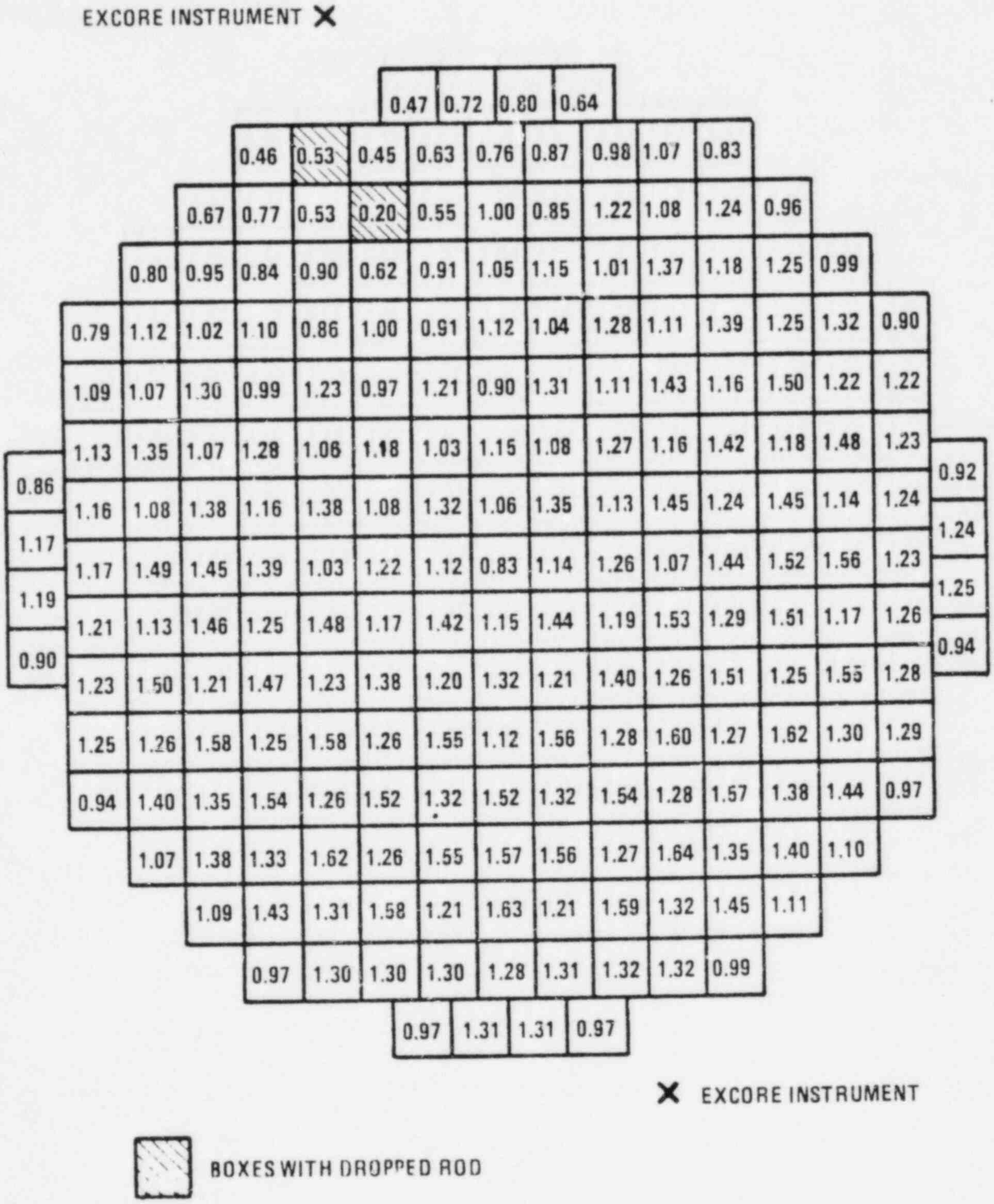

FIGURE 7: EFFECT OF ROD DROP ON ONE PLANE OF POWER SHAPE

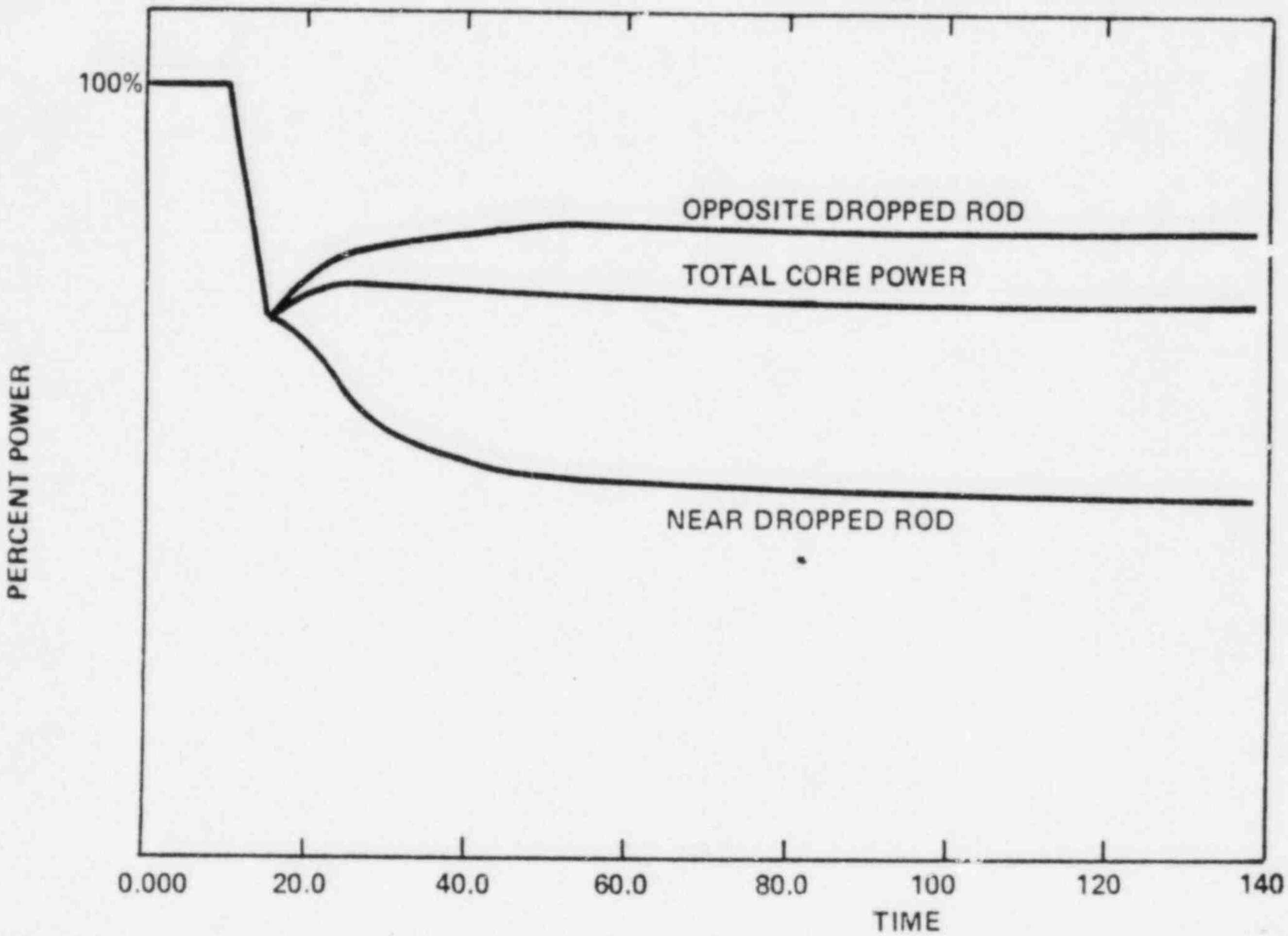

FIGURE 8: EFFECT OF ROD DROP ON EX-CORE DETECTOR SIGNALS

							0.83	1.12	1.12	0.83						
				0.84	1.13	1.13	1.12	1.10	1.12	1.13	1.13	0.85				
			0.95	1.25	1.14	1.37	1.05	1.41	1.05	1.37	1.14	1.25	0.96			
		0.95	1.21	1.17	1.41	1.10	1.35	1.36	1.35	1.10	1.42	1.17	1.22	0.96		
	0.84	1.25	1.19	1.36	1.11	1.34	1.15	1.33	1.16	1.34	1.12	1.37	1.20	1.26	0.85	
	1.13	1.13	1.41	1.11	1.41	1.12	1.38	0.99	1.38	1.13	1.42	1.12	1.43	1.15	1.14	
	1.13	1.36	1.10	1.34	1.12	1.25	1.09	1.19	1.09	1.26	1.13	1.35	1.11	1.39	1.15	
0.83	1.12	1.05	1.35	1.16	1.38	1.09	1.32	1.06	1.32	1.09	1.39	1.17	1.37	1.07	1.15	0.85
1.11	1.10	1.41	1.38	1.33	0.99	1.18	1.08	0.79	1.08	1.20	1.01	1.35	1.42	1.45	1.14	1.15
1.11	1.12	1.05	1.36	1.16	1.39	1.10	1.33	1.07	1.34	1.12	1.42	1.20	1.40	1.09	1.16	1.15
0.83	1.13	1.37	1.11	1.35	1.13	1.27	1.11	1.22	1.12	1.30	1.17	1.40	1.15	1.43	1.18	0.86
	1.13	1.14	1.43	1.13	1.43	1.15	1.41	1.02	1.43	1.17	1.48	1.17	1.49	1.19	1.19	
	0.85	1.26	1.21	1.38	1.13	1.37	1.19	1.38	1.20	1.41	1.17	1.44	1.26	1.32	0.89	
		0.96	1.23	1.19	1.44	1.13	1.39	1.41	1.41	1.16	1.50	1.24	1.29	1.01		
			0.97	1.27	1.16	1.41	1.08	1.47	1.10	1.44	1.20	1.33	1.01			
				0.86	1.16	1.16	1.16	1.15	1.18	1.19	1.20	0.90				
							0.87	1.17	1.18	0.88						

FIGURE 9: EFFECT OF 20 F INLET TILT ON ONE PLANE OF POWER SHAPE